UNIVERSITÀ DEGLI STUDI DI NAPOLI FEDERICO II

FACOLTÀ DI INGEGNERIA

CORSO DI LAUREA IN INGEGNERIA CHIMICA

Tesi di Dottorato di Ricerca in Ingegneria Chimica

MODELLAZIONE DELL'INQUINAMENTO ATMOSFERICO DI ORIGINE VEICOLARE IN DEEP STREET CANYON

Comitato scientifico
Ch.mo Prof. Fabio Murena
Ch.mo Prof. Andrea D'Anna
Ch.mo Prof. Sotiris Vardoulakis

Candidato
Giuseppe Favale

Index

Introduction

During the last 100 years there was an increasing in urbanization all over the world, in most countries it is a natural consequence and stimulus of economic development based on industrialization and post-industrialization. One of the negative effects, related to this, is the increasing of the atmospheric pollution.

Air pollutants are released by a variety of sources, domestic heating, industrial and traffic emissions.

Motor vehicles play a relevant role in the modern industrial economy and in shaping our natural and built environment. Cars and light trucks offer rapid, reliable, and convenient mobility on demand to an ever-growing number of people in countries throughout the world. But for all their positives, automobiles carry with them many negatives. Vehicles are a major source of both air pollution and congested roads, particularly in urban areas, where vehicle concentration is the greatest. They also contribute to global warming, accounting for a large and growing share of greenhouse gas emissions worldwide.

Knowledge of the sources of pollution and the amount of their emission is crucial for developing plans for environmental emission control. In recent years progress has been made in qualification of the environmental damages due to vehicular emissions and the associated costs. These include wide variety of health effects that range from eye irritation, to heart and lung diseases, and even premature death. Particulate emissions also impair visibility, damage ecosystems of national parks, wilderness areas, and water bodies, and could reduce crop production. The pollutants emitted from motor vehicles have a particularly severe impact on the health of the inhabitants, which are now common in most large cities. These include the automobile drivers, pedestrians, as well as people living in the nearby buildings (Nazridoust and Goodarz, 2006).

Vehicles are a major contributor to air pollution around the world. Vehicles account for most of the carbon monoxide (CO), and a large share of the hydrocarbons (benzene, toluene, ethane, ethylene, pentane, etc) (HC), nitrogen oxides (NO_x), and particulates in major urban areas. Much of the effort to reduce pollution from vehicles to date has been in the form of increasingly strict emissions standards on new cars sold in the developed countries. These controls have reduced emissions of CO, HC, and, to a lesser extent, NO_x despite large increases in the number of vehicles and miles driven. Although new cars have become dramatically cleaner over time, many highly polluting vehicles are still on the road, including trucks, busses, motorcycles, and older cars.

Control of gasoline engines and their impact on ambient ozone pollution (NO_x and HC) has been the focus of regulatory efforts in developed countries in the last 20 years, but attention is now turning to emissions from diesel engines. Diesel engines have higher

emissions of NO_x and they have significant emissions of fine particulates. Recent evidence shows that fine particulates may be the most serious threat to human health in urban areas.

CO is a colourless, odourless gas emitted from numerous sources associated with an imperfect fuel combustion (e.g. industrial activities, commercial and home heating, vehicle use). Inhaled CO binds with haemoglobin far more swiftly than inhaled oxygen does, forming carboxyhemoglobin (COHb) and causing hypoxia. Carbon monoxide also binds with myoglobin and mitochondrial cytochrome oxidase, depriving the brain and vasculature of oxygen, so COHb levels alone don't always reflect the severity of toxicity. Tissue hypoxia leads to anaerobic metabolism and lactic acidosis, causing lipid peroxidation and free radical formation-which, in turn, provokes neurotoxicity. Low levels of chronic CO exposure, as from tobacco smoke, industrial CO production, or urban pollution, can affect long-term cardiovascular health by raising blood pressure, encouraging atherosclerosis or thrombotic tendencies, and triggering polycythemia and its increased clotting risk.

NO_x represents the sum of the various nitrogen gases found in the air, of which Nitric Oxide (NO) and Nitrogen Dioxide (NO_2) are the dominant forms. The emission sources are several but all tend to result from high temperature combustion of fuel for industrial activities, commercial and residential heating, and vehicle use. Although most emissions are generally in the form of NO, this nitrogen species can be rapidly converted in the atmosphere to NO_2. NO_2 is felt to be the more significant concern from a human health perspective, being associated with nose, throat and lung effects, and development of air quality standards have focused on this pollutant.

PM is the collective term used to describe a mixture of airborne solid and liquid particles (excluding pure water) with a wide variety of size ranges. Sources of PM are numerous, including both human activity (e.g. industrial stacks, mining pits, vehicles, open burning) and natural (e.g. forest fires, wind blown soil). PM can be both a primary pollutant (directly emitted) and a secondary pollutant (formed through atmospheric chemical reactions). PM is most often differentiated by the size of the particulate.

1 Aim of the thesis

The aim of this thesis is modelling the phenomenon of dispersion of vehicular pollutants in deep and narrow streets, i.e. *deep street canyons*, as function of vehicular emissions and meteorological conditions. At present, the study of deep street canyons is not treated in exhaustive way. As a matter of fact, studies on roads with aspect ratio very close to one ($AR \approx 1$) are more frequently reported. However the old historical centres of many cities, such as Naples, are characterized by narrow streets with $AR > 1$, which are often densely populated with, consequently, high vehicular flows and very high pollution levels.

The study will carried out on a real street canyon in the historical centre of Naples, via Nardones. The choice has fallen just on this place for its geometric configuration that makes it almost an ideal street canyon and for its intensive traffic flow.

In order to rich the aim of this thesis it will necessary to develop a CFD model able to predict, in a good way, the pollutant distribution inside the street canyon as function of meteorological data, background pollutant concentration, traffic intensity and pollution emissions.

For the first thing we have to investigate on the ability of CFD software to model the dispersion mechanism of passive air pollution like CO in deep street canyon. To make this possible we must analyze its features in dealing with complex geometries like that of a deep street canyon and its surrounding area, the ability to deal with multi-specie gas mixture and turbulent flows. Obviously that should be done reaching a good accuracy and precision with a reasonably computational effort. So we need to define a geometrical model able to represent all the main features of the deep street canyon in a not complex way, to make an accurate but not enormous mesh and to choose a numerical algorithm and turbulence closure method accurate but not slow.

After we had set up the model we need to obtain and analyse all the input data necessary, that is meteorological data like wind velocity and direction, traffic intensity and its time distribution, traffic pollutant emission rate and background pollutant concentration.

We need also to analyze how all these input data affect the pollutant concentration level within the canyon and also find the most important ones i.e. those with biggest influence on canyon air quality. To make a good evaluation we must validated the model with measurements obtained in the situ.

CFD models despite their accuracy and precision are a bit onerous, from the computational point of view, and difficult to set up so many empirical or semi empirical models were made up. These are faster than CFD models but are less accurate and usually

are applicable to only a small range of cases because they are made up around those kinds of problems.

Unfortunately almost all this empirical or semi empirical models were made up around regular street canyons so their application on a deep street canyon gives bad results, so we can use our CFD model to make changes to the parametric model in order to simulate the pollutant dispersion in deep street canyons.

2 State of art

Urban air quality is a problem characterized by physical phenomenon which take place into the atmosphere on very different spatial and temporal scales (Soulhac et al. 2003).

The atmosphere is subdivided into five main regions, *troposphere*, *stratosphere*, *mesosphere*, *thermosphere* and *exosphere* each one separated by transition region and identified by the vertical thermal gradient which depend on different fluid dynamic, chemical and radiation phenomenon (Figure 2.1).

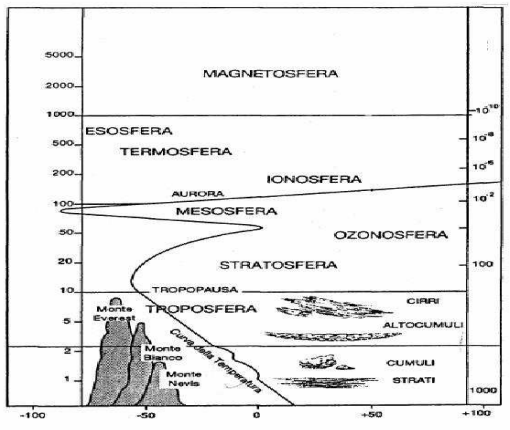

Figure 2.1 Vertical thermal gradient in atmosphere

The troposphere is the nearest region to the ground, the temperature decreases with the height with a rate of about 6.5°C/km up to a minimum of about -50°C at height between 5 and 12 km. The nearest portion of the troposphere to the ground is the *planetary boundary layer* (PBL), which is strongly affected by the temperature variation due to the diurnal irradiation cycle, the viscosity of gases and the ground roughness.

The PBL is the portion of the atmosphere where the generation, decay, transformation and diffusion of most pollutants take place and its thickness, called *friction-layer*, changes during the day reaching the maximum during the morning and minimum during the night.

The turbulence that characterize the PBL has two origins, first the movement of viscous fluids over a rough surface (*mechanical turbulence*), second the heating and cooling of the ground due to the solar radiation during the morning and the ground emission during the night (*convective turbulence*). Therefore the PBL turbulence behaviour

is function of many parameters such as ground roughness, soil radiation feature, atmospheric humidity and wind velocity.

The atmospheric pollutants dispersion is mainly affected by the atmospheric stability which depends on the vertical temperature pattern. The atmospheric stability can be characterized by the *adiabatic thermal gradient* that is the rate of variation in temperature with the height of an air particle during an adiabatic movement.

If the air thermal gradient is less negative than the adiabatic thermal gradient air is cooled more slowly compared to the adiabatic case so the pollutants dispersion is blocked (*stable equilibrium*).

If the air thermal gradient equals the adiabatic thermal gradient the temperature of a particle that moves up or down equals the temperature of the surrounding air (*neutral equilibrium*).

If the air thermal gradient is more negative than the adiabatic thermal gradient air is cooled more quickly compared to the adiabatic case so the pollutants dispersion is enhanced (*unstable equilibrium*).

Pasquill defined six atmospheric stability classes reported in Figure 2.2 , the first one "A" is the most unstable, the forth "D" is the neutral one and "E" and "F" are stable.

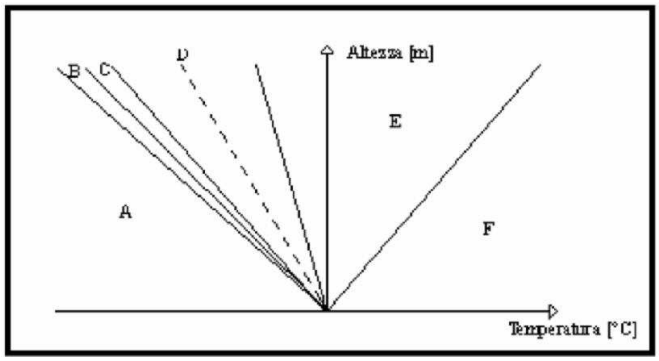

Figure 2.2 Pasquill's atmospheric stability classes

There isn't any model capable of reproducing all the spatial scales that characterize the pollutants dispersion mechanism in urban aria, so it becomes very crucial to construct a modelling system able to represent different phenomenon and scales. We can do this making a *nested model*. There are two different way to construct such modelling system. The first is based on the use of a single three-dimensional Eulerian model nested at different scale using for example the METPHOMOD code or the RAMS code. The second approach is to use different types of models abele to reproduce the physics at different scales.

The local or street scale is generally referred as: *street canyon.* The term *street canyon* has been used originally in order to indicate a relatively tight road lined along both sides

almost continuously from the buildings (Nicholson, 1975). Subsequently the same term has assumed a more wide sense. At first it was extended also to wider roads, for which was coined the appropriate term *avenue canyons*, in order to emphasize the greater amplitude of the street, often followed from a smaller height of the buildings. Later, finally, the term *street canyon* has been reported also to city roads lined from the buildings, also of different height, not necessarily continuously on both sides. Mostly streets that are met in practice, so, if are characterized from the presence of buildings on both sides and from not many crossings with other roads, falls into the current definition of *street canyon*.

After these observations, said *H* the height of the buildings that line the street canyon, *W* the width of the roadway, *L* the length of the street canyon, that is the distance between two crossings along the street axis (Figure 2.3), it's clear that the geometry of a street canyon is essentially characterized through the two ratios (Aspect Ratios) *H/W* and *L/H* between its three characteristic dimensions. For infinitely long *street canyons*, the only geometrical parameter is, obviously, *H/W*, fundamental in the determination of the airflow of the system *street canyon*.

Based on the value assumed by the aspect ratio the street canyons are generally classified in *avenue canyons* (*H/W<0.5*), *regular street canyons* (*H/W≅1*), *deep street canyons* (*H/W>2*).

In the same way the value of the ratio *L/H* allow to distinguish between *short* (*L/H* < 3), *medium* (*L/H* ≅ 5) and *long* (*L/H* > 7) *street canyons.*

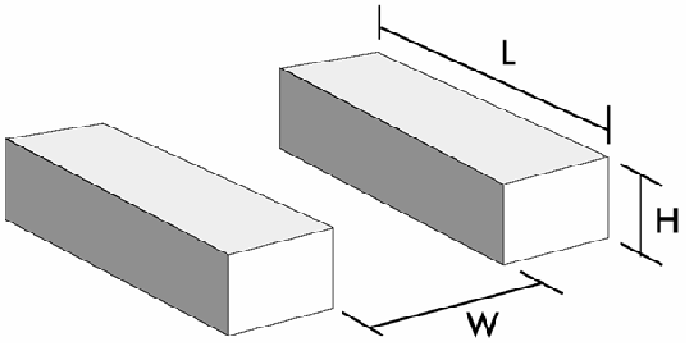

Figure 2.3 Geometric street characteristics

Finally, street canyons lined from buildings of height approximately equal are said *symmetric*, while a meaningful difference between the heights is characteristic of *asymmetric street canyons*. These last ones, then, when the direction of the wind is approximately orthogonal to the street axis, can be subdivided into *step-up canyons*, when the building leeward is higher than that windward, and *step - down canyons* in the contrary case.

Field measurements as well as, numerical and experimental models have been used for studying airflow and pollutant dispersion in street canyons, after that we report some studies and their results that explain the basic aspects of this matter and identify the main parameters and their influence.

According to Vardoulakis et al. (2003) three different dispersion conditions for different wind velocities can be identified. These are: *low wind* conditions for wind speed lower than 1.5 m/s, *perpendicular or near-perpendicular flow* for wind speed over 1.5 m/s blowing at an angle more than 30° to the canyon axes, and *parallel or near-parallel flow* for wind speed over 1.5 m/s blowing at an angle less than or equal to 30° to the canyon axes.

In the perpendicular flow condition the flow may be described in terms of three regimes, depending on the value of the aspect ratio (Oke, 1988): (a) *isolated roughness flow*, (b) *wake interference flow*, and (c) *skimming flow*.

When the buildings are well apart, (H/W<0.3), the wind has sufficient distance to travel from the first building before encountering the next obstacle (Figure 2.4.a), the wakes aren't disturbed and each building is like an isolated obstacle, the flow regime is known as *Isolated Roughness Flow* (IRF).

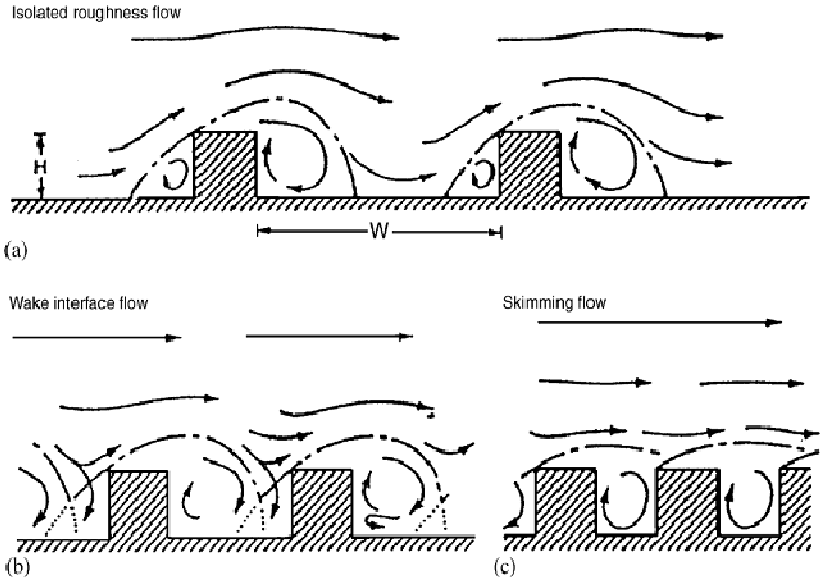

Figure 2.4 : Perpendicular flow regimes in urban canyons for different aspect ratios (Oke, 1988)

When the distribution of buildings becomes more dense (H/W ≅ 0.5) the disturbed air flow has insufficient distance to readjust before encountering the down-wind building the regime changes to one referred to as *Wake Interference Flow* (WIF), (Figure 2.4.b).

At even greater *H/W* a stable circulatory vortex is established in the canyon because of the transfer of momentum across a shear layer of roof height, and transition to a *Skimming Flow* (SF) regime occurs where the bulk of the flow does not enter the canyon, (Figure 2.4.*c*).

Oke (1988), starting from work of Hussain and Lee (1980), made different wind tunnel experiments varying H/W and L/H ratios and found the three different wind regimes and the conditions of transition (Figure 2.5).

Sini et al (1996), using the CHENSI code, studied the case of an infinitely long street canyon investigating the influence of the inverse of the aspect ratio (*W/H*) and the temperature difference between the surfaces of the canyon on airflow structure and pollutant dispersion. Sini at al. (1996) found that the transition from SF to WIF begins at *W/H≈1.5*, but the transition from WIF to IRF is less clear and begins at *W/H≈8-9*.

The SF regime includes two sub-regimes: the first one with a single vortex driven by ambient airflow (*W/H>0.6*) and a second with two or three vortices (*W/H<0.6*).

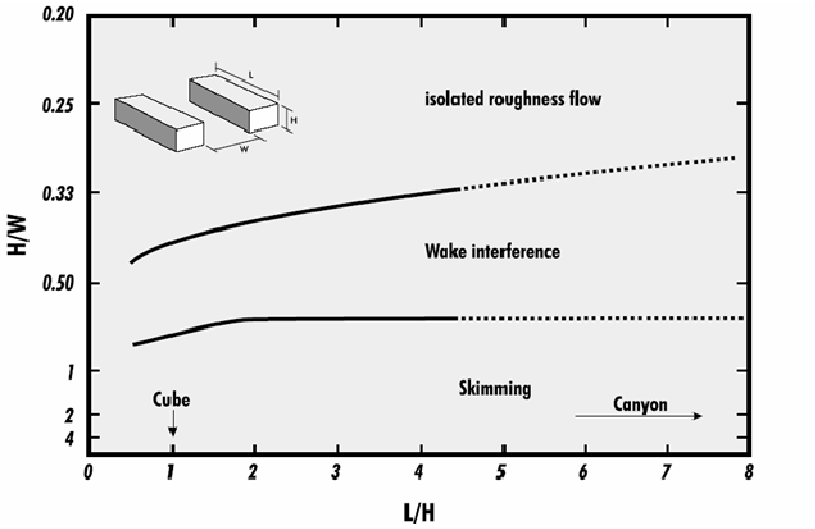

Figure 2.5 The flow regime associated with air flow over building arrays of increasing H/W. The transitions between these three regimes occur at critical combinations of H/W and L/W. (from Oke 1998)

The case of two vortices is characterised by the transport of pollutants by turbulent diffusion in the upper part of the street canyon due to the high turbulence intensity of the upper vortex and their stagnation in the bottom part due to the presence of the weak vortex. In this case there's a worsening of the air quality.

Sini at al. (1996) investigated the influence of the wall temperature on the vertical flow exchange of air in the street canyon and with the air above the roof top level. They found that if the street surface or the up-wind wall are hot the thermal buoyancy increase the vortex intensity and the capacity of air exchange. If the temperature of the down-wind wall is higher than that of the others surface the thermal buoyancy decreases the vortex intensity and split the vortex, so there's a transition from the SF regime with a single vortex to the SF regime with two vortices.

Wind direction at roof top level significantly affects pollutant concentration field within the street canyon. If the wind blows with a direction different from the orthogonal one a spiral flow is induced inside the canyon and the wind component parallel to the street axis becomes the dominant pollutant transport mechanism. Kastner-Klein and Plate (Savory at al. 2004) studied this phenomenon making different analysis in a wind tunnel on a simplified street model (Figure 2.6).

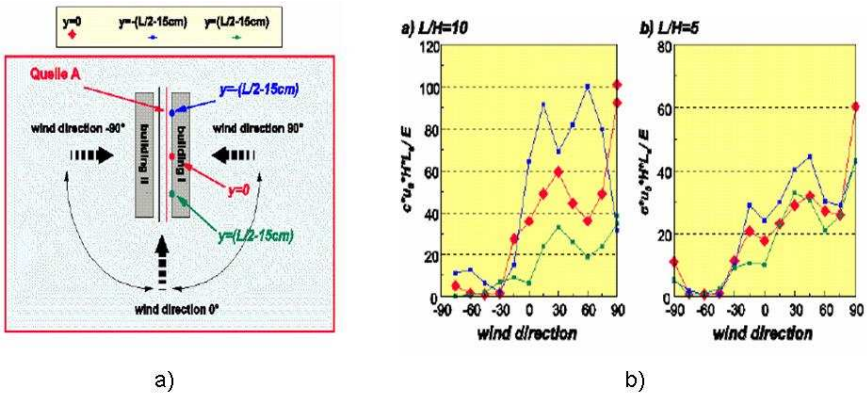

a) b)

Figure 2.6 Evolution of the non-dimensional with the wind direction (from Savory at al. 2004)

They obtained that for a deviation of only 15° from the orthogonal direction the pollutant concentration becomes larger close to the downwind side than in the centre of the street especially if the canyon is long (L/H = 10).

An important improvement to understand the pollutant transport phenomena inside a *street canyon* consists in studying the effect of the nearest buildings on the velocity field.

The presence of one or more upstream buildings deviates the flow field above the street canyon decreasing the street ventilation and worsening the air quality. Kastner-Klein and Plate (Savory at al. 2004) using a simplified wind tunnel model showed that the pollutant concentration within a street canyon, both close to the leeward and the windward wall, increases if one or two upstream buildings are considered.

The presence of a taller or smaller building near a street canyon could be very important because the fluid flow within the canyon could radically change. In the case of a *step-up notch* with a smaller upwind building or a taller downwind one, the fluid flow is

slightly affected and the canyon ventilation is enhanced. In the case of a *step-down notch*, instead, the fluid flow within the canyon strongly changes with a worsening of the air quality. Numerical simulations show that the fluid flow, in a regular street, changes from a one vortex to a two vortex regime with a worsening of the air quality in the bottom part of the canyon (Savory at al. 2004).

The flow and turbulence characteristics inside the urban canopy are highly variable and depend on the building architecture and arrangement in the local environment. It is therefore very difficult to parameterize urban-canopy flow, so a large number of studies were carried out using different *street canyon* configuration (Figure 2.7):

(a) Isolated 2-D street canyon
This approach has the advantage that the boundary conditions can be well defined but has the disadvantage of producing somewhat unrealistic urban flow and dispersion patterns.

(b) Rows of 2-D street canyons
This approach is used in order to understand where street canyon pollution resembles an urban situation. A disadvantage is that the flow, turbulence, and dispersion conditions are determined by the flow separation at the upwind edge of the first building.

(c) The cavity
This is an intermediate case between street canyons of type a) and b), in this configuration there is no first-building effect, but the upwind urban surface is not representative of a rough, irregular building pattern.

(d) Variable roof geometry
Urban buildings do not usually have a simple rectangular geometry in this case Buildings with pitched roofs as well step-down or step-up configurations (upwind building higher or lower than downwind building) were considered.

(e) Nonuniform geometry
Buildings of variable geometry are arranged on staggered or non-staggered arrays, which simulate the rough, irregular pattern of urban landscapes.

(f) Real urban surfaces
This is the most realistic modelling approach for urban street canyons.

A vortex-type motion and associated reverse flow in the lower part of the canyon have been observed in isolated as well as in urban-type idealized canyons with flat roofs.

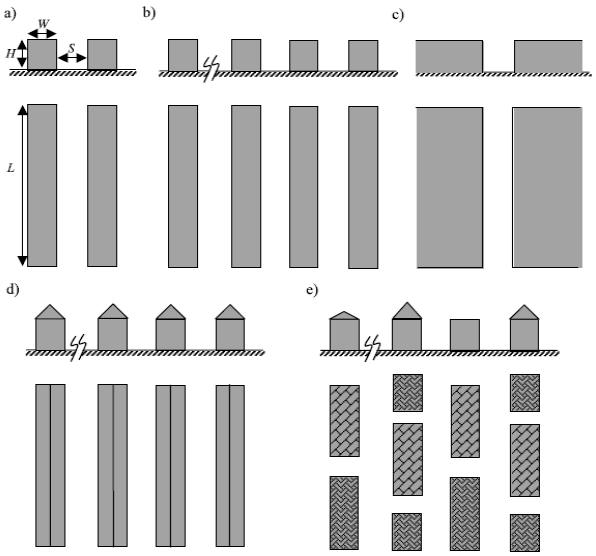

Figure 2.7: Representation of idealized street canyon configurations with increasing complexity (from Kastener-Klein (1998))

Canyons formed by pitched-roof buildings could be characterized by very different fluid flow compared to canyons with flat roofs and fluid dynamic, inside the canyon, strongly depends on the shape of the roofs. Kastner-Klein and Plate (Savory at al. 2004) showed that a downwind pitched-roof building does not significantly affect the canyon ventilation (Figure 2.8 a), while the presence of an upwind pitched-roof building strongly worsens canyon air quality because the strength of vortex inside the canyon decreases very much (Figure 2.8 b).

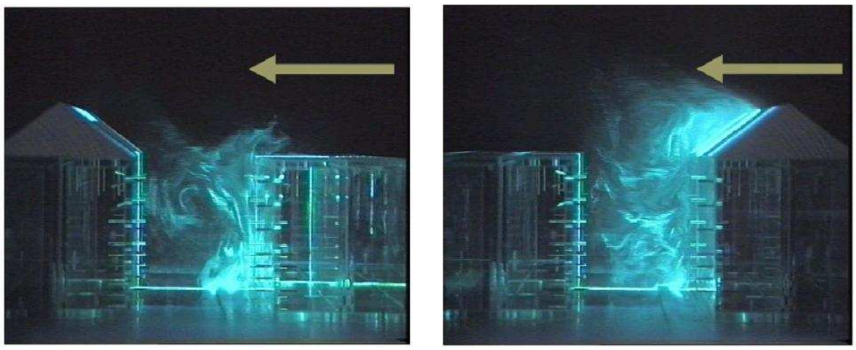

a) b)

Figure 2.8 Street canyon flow patterns in a wind tunnel analysis (From Kastener-Klein)

Vortex type flow has also been observed inside a street canyon within a detailed model of a real urban canopy cluster although less pronounced than in the case of idealized buildings with flat roofs.

In summary, the results from several recent experimental and numerical studies have shown that flow modifications inside street canyons that can be attributed to variations in roof geometry are not negligible. They affect the in canyon vortex formation and dynamics as much as the aspect ratio value does (Kastner-Klein et al, 2004).

Typical street canyons are widely characterised by low airflow intensity, so traffic-induced flow and turbulence plays a significant role. Moving vehicles intensify both micro- and large-scale mixing processes in the environment by inducing turbulence and enhancing advection by entraining masses of air in the direction of vehicle motion. Isao at al. (2006) making different wind tunnel analysis both on a car and a small-size truck model showed that the exhaust gas dispersion is enhanced significantly by the vehicle wake. Car and small-truck promote dispersion both in the horizontal and vertical direction.

Fluid flow modelling of this phenomenon and its effect on the concentration distribution of pollutants are very difficult, particularly the estimation of turbulence field due to vehicle motion.

Plate (1982) suggested that the ratio of turbulence kinetic energy (TKE) due by traffic and wind is a similarity criterion for the wind tunnel modelling of the dispersion of gas pollutant in street canyons. Considering a characteristic flux velocity U and length L, a source emission intensity E and the pollutant concentration c, the dimensionless pollutant concentration c*=cUL/E is equal in the canyon and in the wind tunnel if P_T is the same. The dimensionless concentration c* depends only on P_T and so the problem is to express it by well-known or measurable parameters.

According to Kastener-Klein (1998) the energy production for unit length P_T could be defined as:

$$P_T = \frac{\rho C_{DT} A_T n_T v_v^{\ 3}}{BH'} \qquad 2.1$$

where ρ is the air density, C_{DT} is the drag coefficient, A_T the vehicle frontal area, v_v the average velocity of the vehicles, n_T the number of vehicles per unit length, B the canyon width and H' is a characteristic height.

Jicha et al (2000) studied the pollutant dispersion problem in street canyons in which the traffic flow is significant like road tunnels, large city crossroads and street canyons using a numerical approach based on an Eulerian-Lagrangian method.

This method consists of the replacement of these discrete objects with a continuously moving flow of blocks with a specified velocity and mass. The blocks that represent a vehicle pass through the set of particular control volumes of the solution domain. Assuming a high vehicle Reynolds number and a negligible ratio of density of air and the vehicle, Lagrangian equation for the change of velocity of the vehicle can be written as follows:

$$m_p \frac{d\vec{U}_p}{dt} = \frac{1}{2}\rho_\infty C_D A_p \left|\vec{U}_\infty - \vec{U}_p\right|\left(\vec{U}_\infty - \vec{U}_p\right) \qquad 2.2$$

Where m_p, $\vec{U}_p$ and Ap are mass, velocity and cross section of moving objects, ρ_∞ is density of air, CD is drag coefficient, $\vec{U}_\infty$ is velocity of the ambient air and t is time.

The set of equations for the conservation of mass, momentum, energy and passive scalar is solved for the steady, incompressible turbulent flow. The standard k–ε model of turbulence is employed. The equation for a general variable Φ has the form:

$$\frac{\partial}{\partial x_i}(\rho u_i \phi) = \frac{\partial}{\partial x_i}\left(\Gamma \frac{\partial \phi}{\partial x_i}\right) + S_\phi + S_\phi^p \qquad 2.3$$

Variable Φ stands for velocity components, temperature or enthalpy and concentrations, S_ϕ^p is an additional souse term resulting from the interaction between continuous phase of ambient air and discrete moving objects.

The governing equations for the continuous and discrete phase were solved using the commercial CFD code StarCD based on the finite volume procedure. Jicha at al. (2000) found that on the street axis and near the up-wind wall the dimensionless concentration depends more from the vehicular flux rather than from the wind velocity.

3 Traffic pollution models

As already reported the knowledge of pollutant fields in street canyons is strongly related to the knowledge of the fluid dynamic and dispersion mechanisms. As shown by different observations and wind tunnel studies the fluid flow field in the *street canyons* is strongly characterized by the presence of turbulent vortexes that turn in opposite way and that are the main cause of mass, momentum, energy and pollutants exchange between the canyon and the atmosphere.

In order to model these phenomenon we can use the *Navier-Stokes* equations that are the mathematical formulation of the mass conservation principle, the second principle of dynamic (balance of momentum) and the first principle of thermodynamic (energy conservation). These equations are very difficult to solve being them strongly non linear and this aspect is also the cause of the turbulence phenomenon.

At present there are many ways to model turbulent flow which are characterized by different mathematical or physical principles. So we can distinguish two categories, the numerical models based on the numerical solution of the *Navier-Stokes* equations and semi-empirical models based on a simplification of the problem.

Three are the main ways to model turbulence in numerical models: "*Direct Numerical Simulation*" (DNS), "*Large Eddy Simulation*" (LES) and "*Reynolds Averaged Navier Stokes*" (RANS).

The DNS method consists in solving the complete set of *Navier Stokes* equations without any turbulent model, so this approach solve the complete rang of spatial and temporal scale. It means that the only limitation to accuracy is done by the numerical method used. On the other hand, this approach is very onerous and it can be used only in very simple cases.

The LES approach, born in 1970s to model the atmospheric turbulence, only solves the biggest spatial scales and models the smallest. This approach is based on two observations: first the turbulent kinetic energy of the fluid is mainly carried by the biggest scales; second the smallest scales have a universal behaviour and they can be easily modelled. This approach is very good, but very onerous to apply to a complex three dimensional case such as the fluid dynamic of deep street canyons.

The last approach to turbulence modelling is based on the solution of a set of equations (RANS) obtained from *Navier Stokes* equations averaging them in space and time using the *Reynolds* averages (equations 3.1 3.2 3.3).This approach creates new variables so we must introduce other equations to close the problem.

$$\frac{\partial}{\partial x_j} U_j = 0 \tag{3.1}$$

$$\frac{\partial}{\partial t} U_i + U_j \frac{\partial}{\partial x_j} U_i = \left(\frac{\rho - \rho_n}{\rho_n} \right) g_i - \frac{1}{\rho_n} \frac{\partial}{\partial x_i} p - \frac{\partial}{\partial x_j} \overline{u_i' u_j'} + \upsilon \frac{\partial^2}{\partial x_i \partial x_j} \tag{3.2}$$

$$\frac{\partial}{\partial t} \Theta + U_j \frac{\partial}{\partial x_j} \Theta = - \frac{\partial}{\partial x_j} \overline{u_j' \theta} \tag{3.3}$$

Where U_i and P are the fluid mean velocity and pressure, u_i' is the fluctuating velocity, ρ is the fluid density, υ the kinematic viscosity, g_i the component of the gravitational acceleration vector (0,0,-g), Θ mean temperature deviation from an adiabatic reference status and θ the fluctuation of temperature.

Equation 3.2 is not directly solvable because of the presence of the unknowns Reynolds stresses $\overline{u_i' u_j'}$ that we have to model using a *closure method*.

Two main kind of closure method we can use, the first is the *eddy-viscosity* while the second is the *higher closure method* which involves the introduction of new equations to model the Reynolds stresses (Reynolds Stress Model, RSM).

The eddy viscosity method assumes that the Reynolds stresses are proportional to the local velocity gradients, as happens for molecular diffusion, so:

$$\overline{u_i' u_j'} = -\upsilon_t \left[\frac{\partial u_i}{\partial x_j} + \frac{\partial u_j}{\partial x_i} \right] \tag{3.4}$$

$$\overline{u_j' \theta} = -K_t \frac{\partial \Theta}{\partial x_j} \tag{3.5}$$

Where υ_t is the eddy kinematic viscosity that actually is a tensor but in most engineering application is considered a scalar quantity and K_t is the turbulent eddy diffusivity which is related to the υ_t through the turbulent Prandtl number $Pr_t = \upsilon_t / K_t$ that is approximately constant ($Pr_t \approx 0.7$).

The most used method in practical cases is the so called κ-ε model which introduces two new equations to model the turbulence. This method assumes that υ_t is proportional to a velocity length scales obtained from the turbulent kinetic energy

$$k = \frac{1}{2}\overline{u_i' u_i'} \tag{3.6}$$

and the turbulent dissipation rate

$$\varepsilon = \nu \overline{\frac{\partial u_i'}{\partial x_j}\frac{\partial u_i'}{\partial x_i}} \tag{3.7}$$

So the eddy-viscosity is defined as:

$$\nu_t = c_\mu \frac{k^2}{\varepsilon} \tag{3.8}$$

Where c_μ is an empirically defined constant ($c_\mu = 0.09$).

In the case of *standard* κ-ε model transport equations of κ and ε are obtained from semi-empirical considerations, while a more complicate formulation is possible using the so called *Re-normalization Group* (RNG) method. This latter method try to account for the effect of smaller scales of motion, as matter of fact the standard κ-ε method calculates the eddy viscosity from a single turbulent length scale. The RNG approach, whose application is similar to the standard one, creates a ε equation different from the standard method.

The diffusivity modelling is, obviously, strongly related to the fluid flow modelling and its behaviour is described by the mass conservation scalar equation:

$$\frac{\partial C^\alpha}{\partial t} + U_j \frac{\partial C^\alpha}{\partial x_j} = -\frac{\partial \overline{u_j' c}}{\partial x_j} + S \tag{3.9}$$

Where C^α is the mean concentration of passive pollutant α and S represents all sources or sinks.

Using the eddy diffusivity approach the turbulent flux terms $\overline{u_j' c}$ should be modelled as:

$$\overline{u_j' c} = -K_c \frac{\partial c}{\partial x_j} \tag{3.10}$$

Where K_c is the eddy diffusivity coefficient which is related to the υ_t through the turbulent Schmidt number $Sc_t = \upsilon_t / K_c$ that is approximately constant ($Sc_t \approx 0.9$).

Another approach is based on the stochastic Lagrangian trajectory model, where concentrations of pollutants are obtained calculating the movement of particles representing air parcels. The trajectories are calculated using the mean flow field adding random fluctuations whose statistic depends on the mean fluid field.

All these numerical models commonly called CFD are very useful for research purpose because of their accuracy, and there are also many commercial or homemade code such as FLUENT, StarCD, CFX, but they are still too complex for practical purpose such as support of air pollution management. So many parameterized semi-empirical models are made using simplifications and assumptions on the fluid flow model and dispersion mechanism. The best known are the STREET model, the Hotchkiss and Harlow model, the CPBM and the OSPM model.

The STREET model is one of the earlier street pollution models and is empirically derived from measurements on streets carried out in San Jose and St. Louis. This model assumes that the concentration of pollutant is made by the sum two amounts, the first coming from street traffic emissions (c_s) the second from background concentration (c_b):

$$c = c_s + c_b \tag{3.11}$$

The street component is proportional to the street emissions Q [$gm^{-1}s^{-1}$] and inversely proportional to the roof level wind speed *u*. For wind blowing with an angle bigger than 30° to the street direction the concentration for the leeward and windward side of the street are respectively:

$$c_s = \frac{K}{u + u_s} \sum_i \left[\frac{Q_i}{\left(x_i^2 + z^2\right)^{0.5} + h_0} \right] \tag{3.12}$$

$$c_s = \frac{K}{u + u_s} \frac{H - z}{H} \sum_i \frac{Q_i}{W} \tag{3.13}$$

Where K is an empirical constant (K≈7), u_s represent the induced by traffic air movement, h_0 represent the initial mixing of pollutant, x_i and z are the horizontal and vertical distance of the receptor from the i^{th} traffic lane, Q_i is its emission and H and W are the height and width of the canyon.

The *Canyon Plume Box Model* (CPBM) proposed by Yamartino and Wiegand (1986) calculates the pollutants concentrations using a plume model for vehicular emissions and a box model to account pollutants recirculated within the street by the turbulent vortex flow.

The wind flow inside the canyon is obtained using the Hotchkiss and Harlow method for transversal components and a logarithmic profile for the longitudinal component. An empirical model, that takes into account the effects of wind generated turbulence and thermal effects induced by solar radiations and moving vehicles, is used to calculate the standard deviations of the flow velocity components about the mean flow.

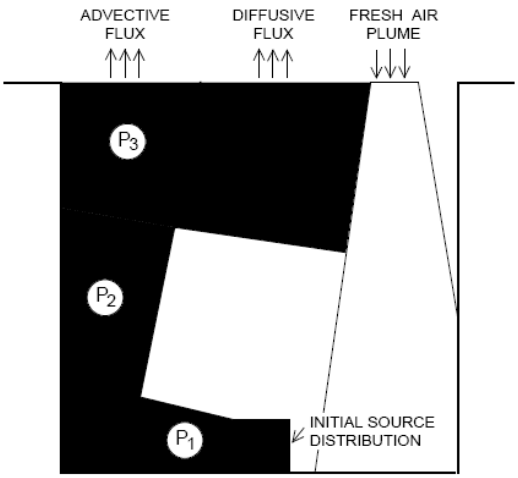

Figure 3.1 Schematic diagram of the principal mechanisms of the vortex sub-model in the Canyon Plume-Box Model (from Yamartino and Wiegand (1986))

As shown by Figure 3.1 the plume inside the canyon is divided into three components (P_1, P_2 and P_3) which follow straight line trajectories and are dispersed according to Gaussian plume formulae. The contribution to concentration obtained from recirculation component is calculated from the mass budget within the canyon by:

$$C_R = \frac{Q}{u_b\left(W/2\right)}\frac{F}{1-F} \qquad 3.14$$

Where Q is the emission rate, W is the canyon width and F is the fraction of material recirculated

$$F = \exp\left(-t_s/\tau\right) \qquad 3.15$$

Where t_s is a time scale related to the vortex recirculation time and τ the life time.

On the leeward side of the street the concentration obtained from the direct plum model is added to the recirculation concentration C_R. On the windward side, where the only contribution comes from the recalculation component, the dilution of the concentration due to the fresh air entrainment is taken into account.

The OSPM model is based on similar principles of the CPBM model, i.e. concentrations of the exhaust gases are calculated using a plum model for the direct contribution and a box model for the recirculating part as reported in Figure 3.2.

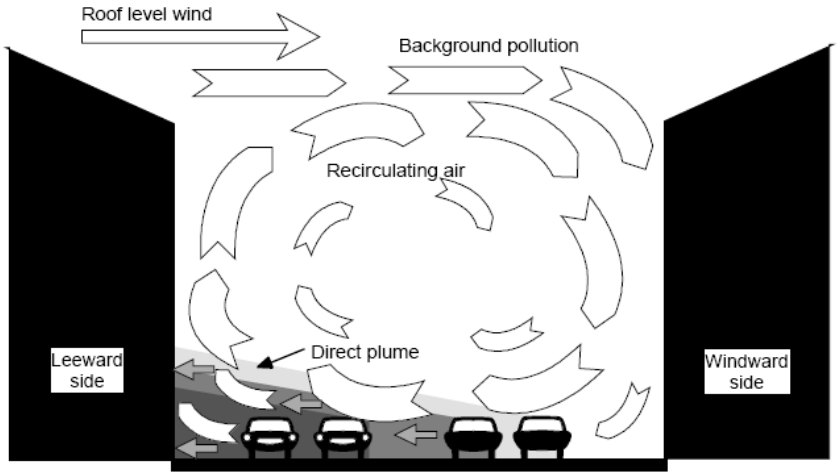

Figure 3.2 Schematic illustration of the basic model principles in OSPM.

OSPM uses a very simplified parameterization of flow coming from extensive analysis of experimental data and model tests.

OSPM assumes that traffic and traffic emissions are uniformly distributed across the canyon and the emission field is treated as a number of infinitesimal line sources perpendicular to the wind at the street level. The emission density for a line is:

$$dQ = \frac{Q}{W} dx \qquad 3.16$$

Where Q is the emission in the street ($gm^{-1}s^{-1}$) and W is the street width.

The contribution to the concentration at a point distant x to the source line is:

$$dC_d = \sqrt{\frac{2}{\pi}} \frac{dQ}{u_b \sigma_z(x)} \qquad 3.17$$

Where u_b is the wind speed at street level and $\sigma_z(x)$ is the vertical dispersion parameter at downwind distance x.

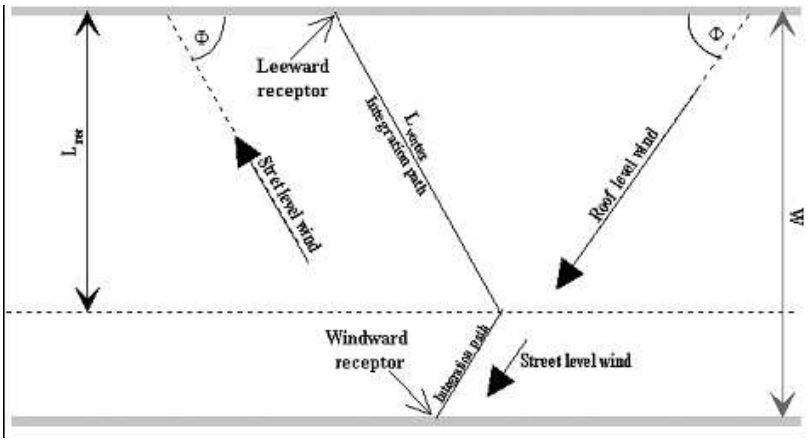

Figure 3.3 Illustration of the wind flow and formation of the recirculation zone in a street canyon

Equation 3.17 is integrated along the wind path which depends on the wind direction, extension of the recirculating zone and the street length. The wind velocity at street level is assumed to be mirror reflected with respect to the roof wind, the length of the vortex (L_v) is assumed twice the height of the upwind building (H_u) and linearly decreasing for velocity with the wind speed for wind speed values less than 2 m/s.

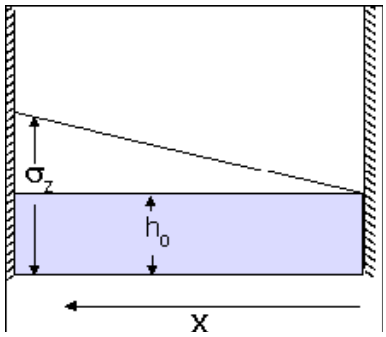

Figure 3.4 Geometrical representation of the vertical dispersion parameter

The vertical dispersion parameter is given by:

$$\sigma_z(x) = \sigma_w \frac{x}{u_b} + h_0 \qquad 3.18$$

Where σ_w is the vertical turbulence velocity fluctuation depending on the wind and traffic turbulence and h_0 is the initial dispersion wakes of the vehicles ($h_0 \approx 2 - 4$ m).

For a special case of wind direction perpendicular to the street axis the direct contribution to the concentration is:

$$C_d = \sqrt{\frac{2}{\pi}} \frac{Q}{W\sigma_w} \ln\left(\frac{h_0 + \left(\sigma_w / u_b \right)}{h_0} \right) \qquad 3.19$$

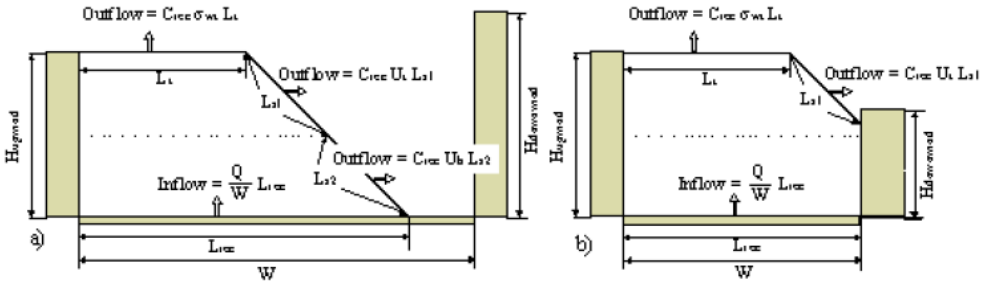

Figure 3.5 Geometry of the recirculation zone.

The recirculation contribution is calculated using a simple box model (Figure 3.5), assuming that the canyon vortex has the shape of a trapeze and the maximum length upper edge been half of the vortex length.

The inflow rate per unit length and the outflow rate are:

$$INFLOW = \frac{Q}{w} L_{rec} \qquad 3.20$$

$$OUTFLOW = C_{rec}\left(\sigma_{wt} L_t + u_t L_{S1} + u_b L_{S2} \right) \qquad 3.21$$

Were L_{rec} is the width of the recirculating zone, σ_{wt}, u_t and u_b are the flux velocity from the top and siding edges.

The concentration in the recirculating zone is calculated assuming that inflow rate equals the outflow rate and that the pollutants are well mixed inside the zone. In the simple case when the vortex is totally immersed inside the canyon (AR = H/W $\geq$ 1) the recirculation contribution is:

$$C_{rec} = \frac{Q}{\sigma_{wt} W} \tag{3.22}$$

The wind speed at street level, u_b, is calculating assuming a logarithmic reduction of the wind speed at roof level towards the bottom of the street:

$$u_b = u_t \frac{\ln(h_0 / z_0)}{\ln(H / z_0)} (1 - 0.2\, p \sin(\Phi)) \tag{3.23}$$

Where H is the average depth of the canyon, h_0 is the initial dispersion height, z_0 the roughness length and $p = H_{upwind}/H$.

4 The situ of via Nardones

Naples is a densely populated city with 975.139 inhabitants over a surface of about 117 km^2 that means 8,315 inh km^{-2}. The Neapolitan vehicular flit is made from about 543,000 cars, 199,300 two-wheels vehicles and 3,000 buses. The historical centre is quite large and characterized by narrow streets, 5-7 meters wide one way traffic without pedestrian pavements with buildings relatively high (about 25-40 meters).

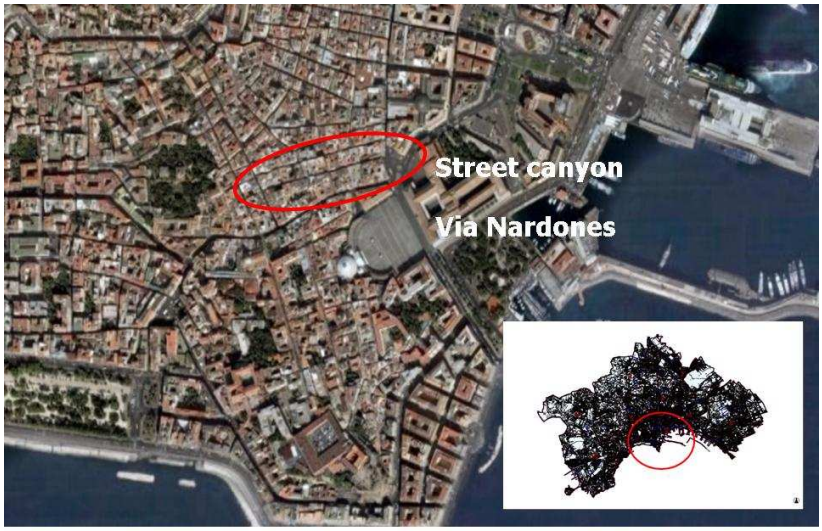

Figure 4.1 The situ of via Nardones

Air quality in the city is monitored by a network of nine fixed stations measuring conventional pollutants (CO, NO_2, NMHC, PM_{10}, O_3 and SO_2). Hourly average concentrations are available for these pollutants and Table 4-1, Table 4-2, Table 4-3, Table 4-4, Table 4-5 and Table 4-6 report some data coming from these stations.

In addition benzene is monitored in 12 sites by passive samplers but in this case only average monthly concentrations are available. An analysis of the air quality in the urban area of Naples was carried out by Murena at al, 2000.

Table 4-1 PM_{10}: Year Average concentration of PM_{10} (threshold value in 2005 DM60/02: 40 $\mu g/m^3$)

Station	Station Type	Area Type	1994	1995	1996	1997	1998	1999	2000	2001	2002	2003	2004	2005
NA01	Background	Suburban											26	22
NA02	Traffic	Urban							70	75		50	44	
NA03	Traffic	Urban							23	43	51	45	21	
NA05	Traffic	Urban							25	41	35	38	31	27
NA07	Traffic	Urban							62	46	35	41	36	31
NA09	Traffic	Suburban											33	33

Table 4-2 PM_{10} Number of days' exciding threshold value of PM_{10} (maximum number allowed in 2005 DM60/02: 35)

Station	Station Type	Area Type	1994	1995	1996	1997	1998	1999	2000	2001	2002	2003	2004	2005
NA01	Background	Suburban											20	13
NA02	Traffic	Urban										42	51	
NA03	Traffic	Urban								56		59	2	
NA05	Traffic	Urban								29	50	82	24	23
NA07	Traffic	Urban								77	45	86	63	38
NA09	Traffic	Suburban											31	32

Table 4-3 O_3: Number of days' exciding threshold value of O_3 (DLgs 183/04)

Station	Station Type	Area Type	1994	1995	1996	1997	1998	1999	2000	2001	2002	2003	2004	2005
NA01	Background	Suburban			17	4	23	17	0	2	0	0	22	5
NA08	Traffic	Urban			1	3	3	2	1	9	1	1	3	1
NA09	Traffic	Suburban			0	8	3	7	6	4	1	0	8	5

Table 4-4 NO_2: Year Average concentration of NO2 (threshold value in 2010 DM60/02: 40 $\mu g/m^3$)

Station	Station Type	Area Type	1994	1995	1996	1997	1998	1999	2000	2001	2002	2003	2004	2005
NA01	Background	Suburban	42	42	41	37	28	47	51	50	54	53	32	28
NA02	Traffic	Urban	61	71	67	65	61	66	65	45	58	51	37	43
NA03	Traffic	Urban	54	50	53	59	48		60	44	65	47	30	48
NA05	Traffic	Urban	67	100	83	68	103	76	77	94	59	61	33	40
NA07	Traffic	Urban	95	119	101	108	158	104	133	110	88	72	46	70
NA08	Traffic	Urban			73	59	43	36	63	62	50	56	38	28
NA09	Traffic	Suburban			30	61	105	67	65	36	36	39	38	29

Table 4-5 NO_2: Number of hours' exciding threshold value of NO_2 (maximum number allowed in 2010 DM60/02: 18)

Station	Station Type	Area Type	1994	1995	1996	1997	1998	1999	2000	2001	2002	2003	2004	2005
NA01	Background	Suburban											2	0
NA02	Traffic	Urban	40	190	93	123	127	5	7	5	2	2	6	2
NA03	Traffic	Urban	15	116	51	59				8	119	15	0	0
NA05	Traffic	Urban											6	0
NA07	Traffic	Urban	287	786	467	769	1799	774	1650	734	193	5	0	20
NA08	Traffic	Urban				29	33	0	181	190	75	150	1	0
NA09	Traffic	Suburban				352	468	381	308	40	27	39	20	15

Table 4-6 SO_2: Number of days' exciding threshold value SO2 (threshold value in 2005 DM60/02: 3)

Station	Station Type	Area Type	1994	1995	1996	1997	1998	1999	2000	2001	2002	2003	2004	2005
NA01	Background	Suburban											0	0
NA09	Traffic	Suburban											0	0

Source of data: ENEA and CRIA/ARPAC – Napoli 2005

The air monitoring network doesn't include any deep street canyon among the monitoring sites, in fact the fixed stations are located in relatively large street with AR ≈ 1. Murena and Vorraro (2003) carried out a monitoring campaign of benzene in a deep street canyon (via Nardones) locating passive samplers at different height and showing that benzene concentration was very high in the deep street canyon considered especially at pedestrian level where it is higher than the threshold limit value of 10 $\mu g m^{-3}$. Other studies (F. Murena and G. Favale, 2007) showed that pollutant concentration in the same street canyon is generally higher than those measured in the monitoring stations located in Naples.

Therefore, in this thesis the same deep street canyon was chosen in order to study the pollutant dispersion in deep street canyons.

Via Nardones is situated in the historical centre of Naples close to the seacoast (Figure 4.1). Its axis is almost oriented in the west-east direction, and is surrounded by via De Cesare at north, via Chiaia at south, via Gradoni di Chiaia at west and piazza Trieste e Trento at east (Figure 4.2). All those streets are very close to via Nardones so they could strongly affect the fluid flow inside the canyon. Via Nardones has also a crossing and a lateral streets that cut it into three parts having length L_1 = 105.0 meters (from via Gradoni di Chiaia to the first crossing street), L_2 = 65.0 meters (between the two crossing streets) and L_3 = 145.0 meters (from the second crossing street to piazza Trieste e Trento) (Figure 4.3). The canyon has a whole length of L = 315.0 meters, it is wide 5.8 meters and all the surrounding buildings have almost the same height that is about 30-35 m meters. On the whole, the ratio between street length and height is L/H = 9.5 and the street could be considered a long street canyon. But intersections must be considered. In this case the three parts have the following L/H ratios: L_1/H = 3.3; L_2/H = 1.8 and L_3/H = 4.2. Therefore, each part could be considered as a short or medium street canyon.

Figure 4.2 the deep street canyon of via Nardones

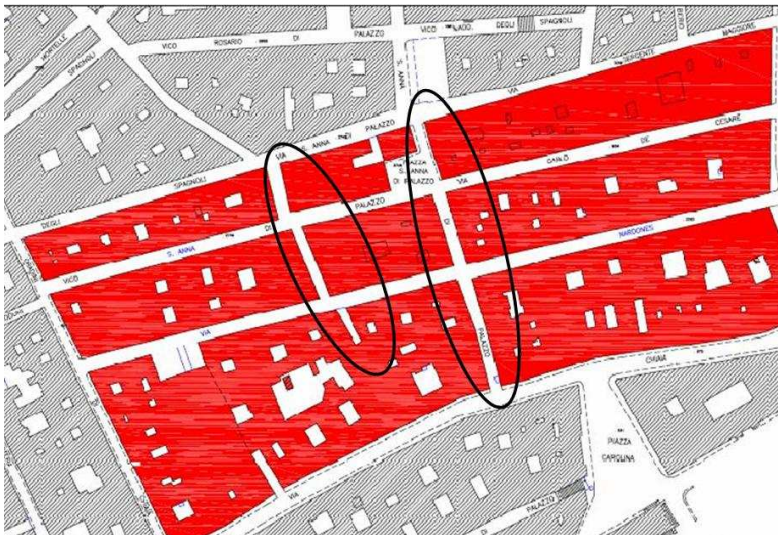

Figure 4.3 via Nardones and its lateral and crossing streets

5 Monitoring campaigns

During the week from 14 to 20 of June 2006 a monitoring campaign of carbon monoxide, inside the street canyon of via Nardones, was carried out in order to analyze the pollutant field and its dynamic during many days (Murena and Favale, 2007). The data obtained allow us to better understand the main dispersion features of a deep street canyon and also give us many useful information to improve and validate a computational model.

The CO concentration was measured at two sampling points, the first located at 2.5 meters height from ground and 1.3 meters from the south wall of the street, representing the concentration at pedestrian level, the second at 25 meters height (Figure 5.1).

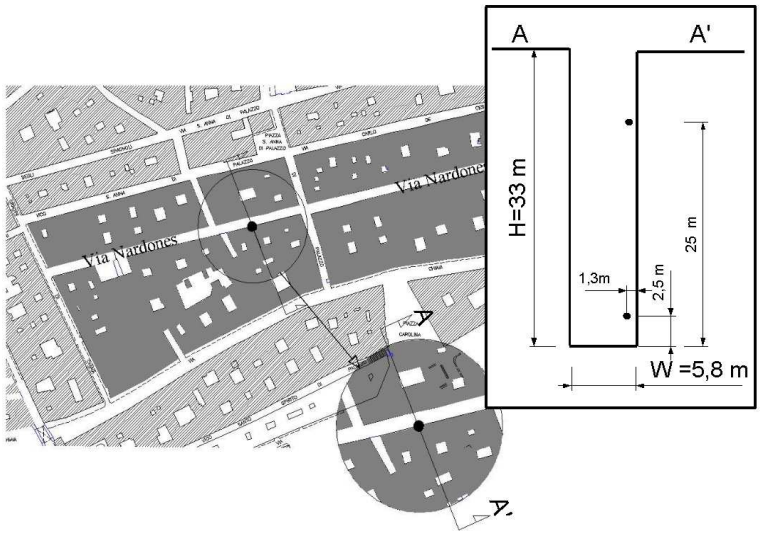

Figure 5.1 Plan view of via Nardones and surrounding streets (left). Cross-section of the street canyon (right) with sampling points. (from Murena F. and G. Favale, (2007))

As reported by Figure 5.2 the concentration, at standard conditions of *T=273.15K* and *P=100kPa*, at the sampling point situated at *2.5 m* height, sometimes exceed the EC limit of *10 mg/m*^{3}. As matter of fact, even though we exceed the limit only 265 times on 9475

values, the concentration inside the canyon could be very high and so very dangerous for people.

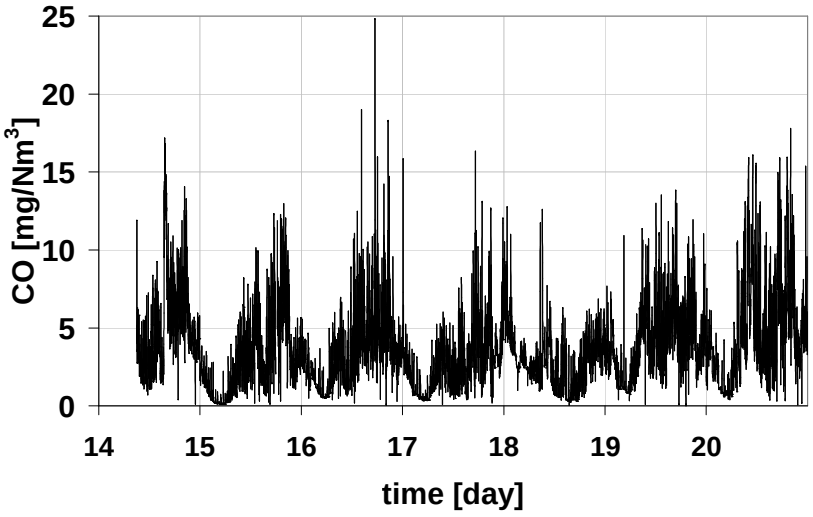

Figure 5.2 Via Nardones: CO concentration levels (one minute average values) measured during the monitoring campaign (14 June-20 June) at h = 2.5 m (from Murena F. and G. Favale, (2007))

At same time if we compare the typical day concentration levels measured by some permanent monitoring stations situated in the urban area of Naples with these data, as reported in Figure 5.3, we can easily understand that a deep street canyon, like this, is a hot spot. As a matter of fact the concentration inside the canyon is higher than concentrations measured in a scarcely urbanized area (NA1) but also is higher than concentrations measured by background stations (NA4, NA7).

As we can see from Figure 5.3 which reports the concentration curves at two sapling points, h=2.5m and h=25m, the concentration at the first point is generally higher than to the second, but between 3 and 7 hours there is an inversion probably due to the very low traffic intensity during these hours in the street canyon.

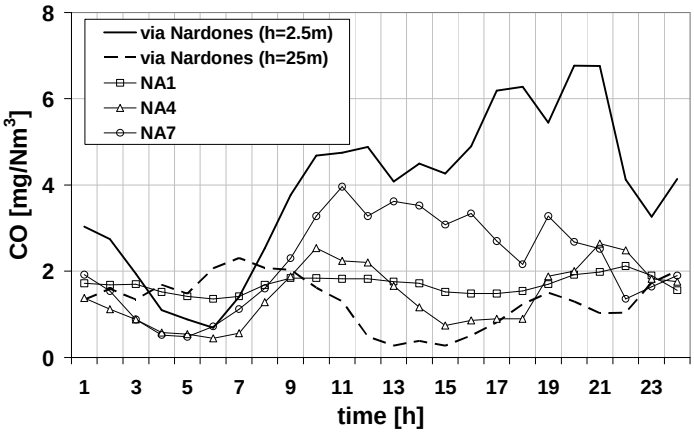

Figure 5.3 Typical day curves of CO concentration levels measured in the deep street canyon (via Nardones h = 2.5 m and h=25 m) and at permanent air quality monitoring stations located in the urban area of Naples (NA1, NA4 and NA7). Data refers to weekdays (Mon-Fri) from 14 to 20 June. (from Murena F. and G. Favale, (2007))

Figure 5.4 reports the relationship between emission rate, obtained through the COPERT method, and concentration at *h=2.5 m*. Obviously the two quantities are related but not completely, which means that other phenomenon, such as meteorology and background concentration, strongly affect the pollution inside the canyon.

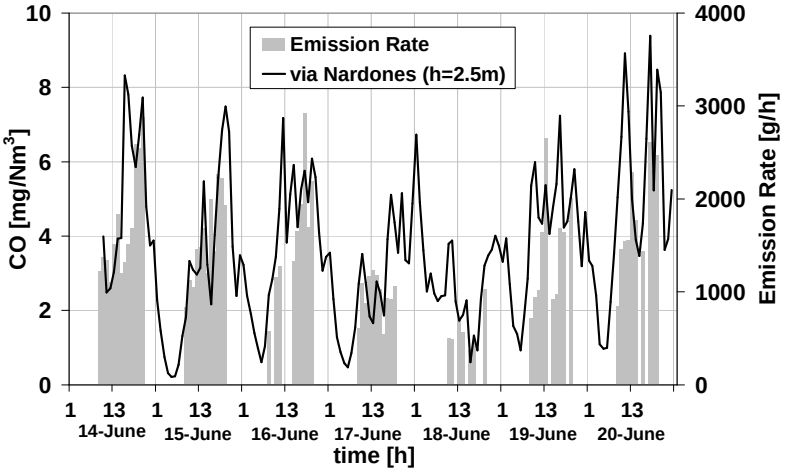

Figure 5.4 Via Nardones: hourly average values of CO concentration level at h = 2.5 m and of CO emission rate evaluated with COPERT procedure (from Murena F. and G. Favale, (2007))

If we compare the mean values of concentration at h=2.5m and emission during weekdays (Monday-Friday), as reported in Figure 5.5, there is a better correlation, this is probably due to the strong simplification of using constant average emission factors for the calculation of emissions, so this method improve with the increasing of vehicles number.

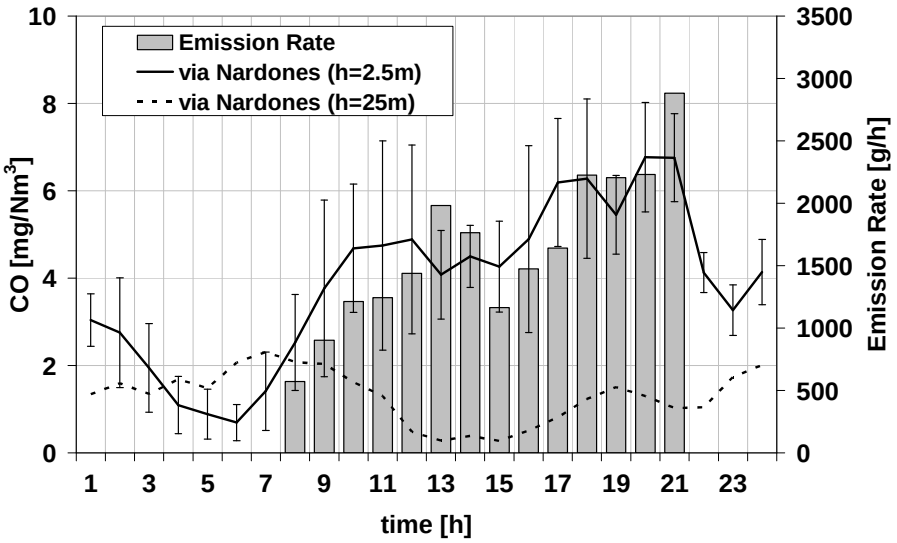

Figure 5.5 Via Nardones: typical day curves in weekdays (Mon-Fri) of CO concentration levels measured at h = 2.5 m, h= 25 m and emission rate (from Murena F. and G. Favale, (2007))

The spatial variability of air pollution in urban areas creates concern about the representativeness of measurements used in exposure studies (Scaperdas and Colvile 1999, Vardoulakis et al. 2002). Moreover, it adds complexity to the development of useful air pollutant dispersion models. Berkowicz et al. (1996) showed that roadside measurements are site-dependent and not representative of the urban area. On a single-street scale, spatial variability has been observed both on a vertical (Vakeva et al. 1999; Chan and Kwok 2000; Vardoulakis et al. 2002, Murena and Vorraro 2003) and horizontal basis (Coppalle et al. 2001, Vardoulakis et al. 2002 and 2005, Tsai and Chen 2004). Horizontal variability has mainly been studied on the direction perpendicular to the street axis. Significant differences in concentrations on the two sides have been detected when wind direction is mainly perpendicular to the street axis (Vardoulakis et al. 2002 and 2005, Tsai and Chen 2004). However, most of these studies are concerned with regular street canyons where the aspect ratio (H/W) is AR $\cong$ 1. If AR $\cong$ 1, and the wind direction is mainly perpendicular to the street axis, an induced vortex-like flow inside the canyon takes place (Sini et al. 1996).

In the case of AR > 1 the flow field inside the canyon changes significantly with respect to AR $\cong$ 1. In addition the vehicle-induced turbulence and other effects like thermal

ones can hinder the formation of the bottom vortex. Therefore, a vortex-like flow could not occur at the road level of a deep street canyon (AR > 1.5-2) and vehicle-induced turbulence would increase mixing in the bottom part of the canyon such that pollutant concentrations on the two sides of a deep street canyon may be assumed the same.

From Monday 16 to Wednesday 18 April 2007 a carbon monoxide monitoring campaign was carried out in via Nardones (Murena at al, 2008). The CO concentration was measured at 2.5 m height from the road pavement and 1.3 m from the wall, using a non-dispersive infrared photometer analyzer (ML 9830B Monitor Europe Ltd with lower detectable limit LDL=0.05 ppm). Sampling started at 9.30 a.m and stopped at 8:30 p.m. The sampling point was shifted each hour from one side of the street to the other (Figure 5.6).

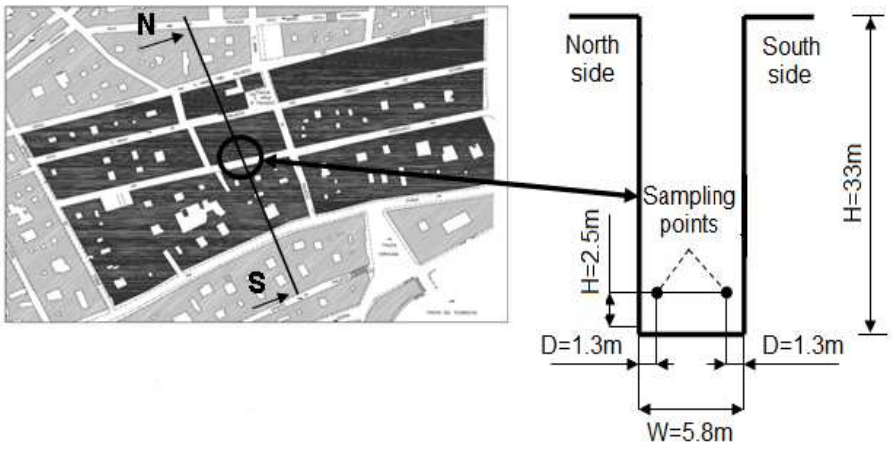

Figure 5.6 Plan view of via Nardones and surrounding streets (left). Cross-section of the street canyon (right) with sampling points. (from Murena F. at al, (2008))

In Figure 5.7 the one-minute average concentrations of CO measured on the north and south sides of Via Nardones from Monday 16 to Wednesday 18 April 2007 are reported. The CO concentration levels measured during the monitoring campaign were generally low, but some spikes were detected. Major spikes occurred on the 16th at 16:15; on the 17th at 15:00 and on the 18th at 18:00. The decrease in concentration after the very rapid increase corresponding to the events reported above, generally took about one hour. This time is consistent with the evaluation of average residence time of pollutants in a street canyon reported by Murena and Ricciardi (2005).

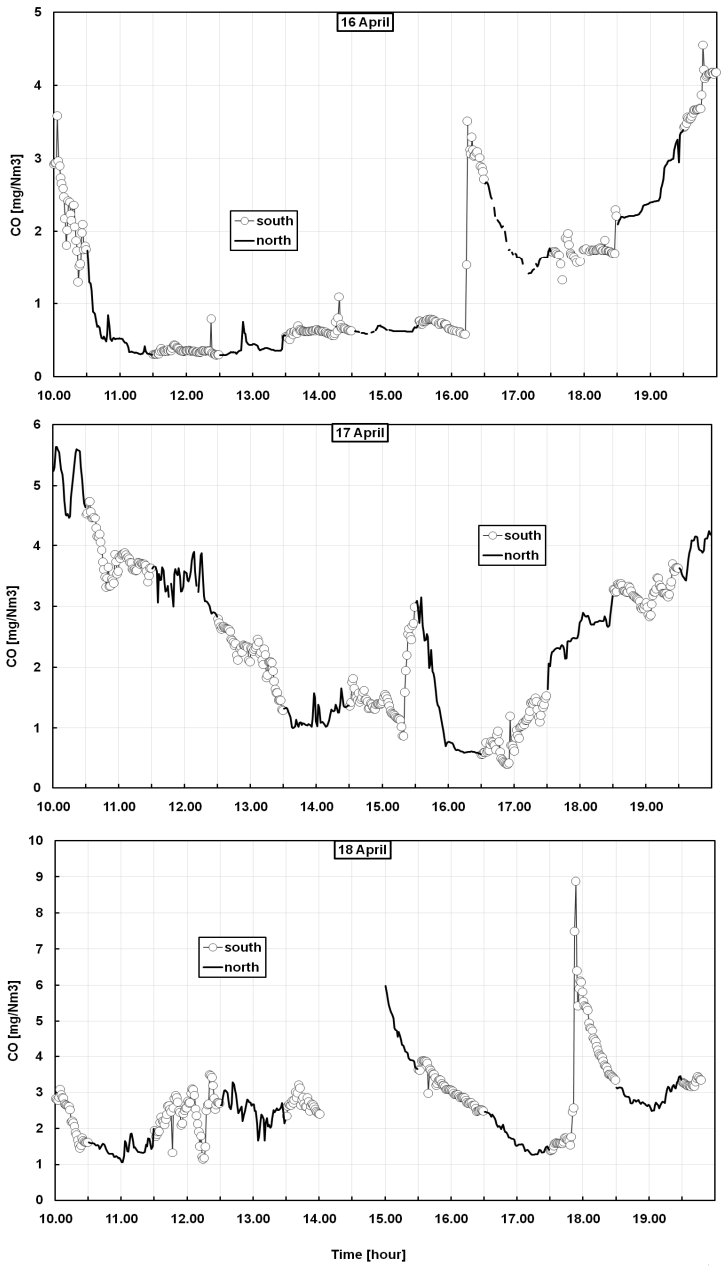

Figure 5.7 one-minute average concentrations of CO measured on the north and south sides of Via Nardones from Monday 16 to Wednesday 18 April 2007 (from F. Murena at al. 2008)

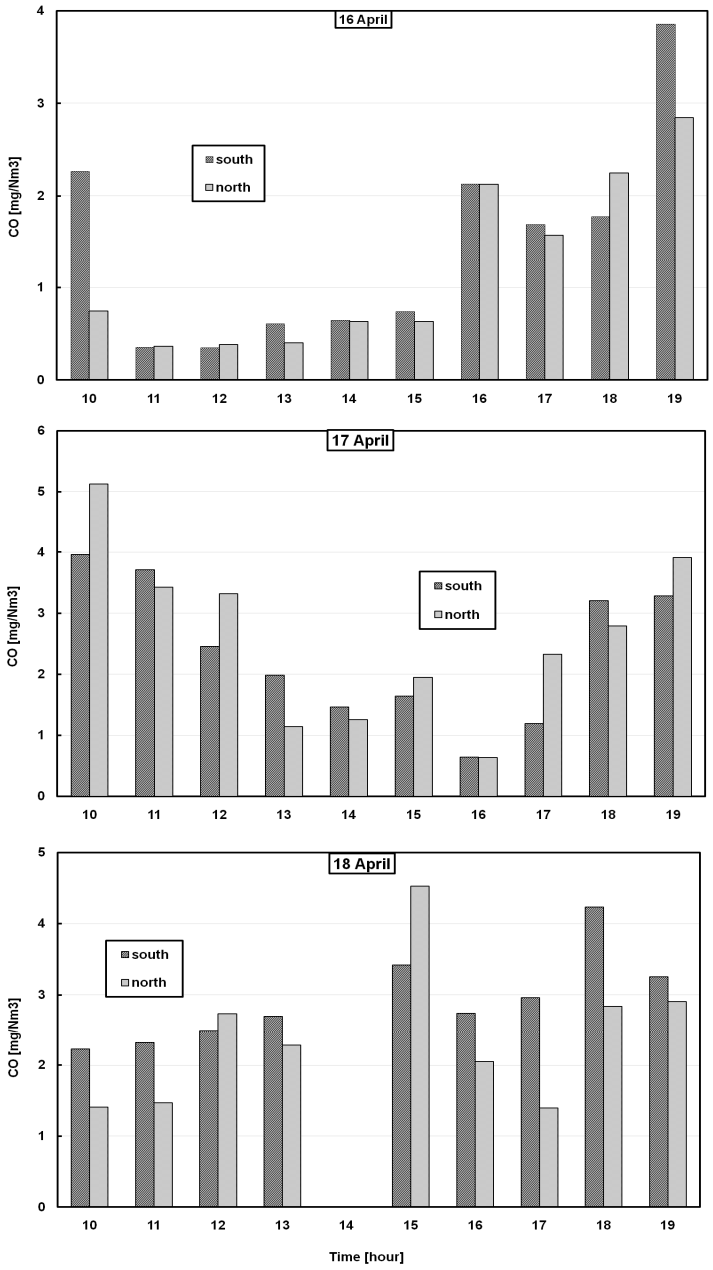

Figure 5.8 Hourly average CO concentrations are reported as histograms (from F. Murena at al. 2008)

On the basis of data reported in Figure 5.7, thirty-minute average CO concentrations, on each side, were evaluated and assumed as hourly average values. Hourly average CO concentrations are reported as histograms in Figure 5.8 where it may be observed that north and south side concentrations are very similar.

Therefore, both Figure 5.7 and Figure 5.8 constitute the first experimental evidence that north and south side concentrations are very similar at the same time. The same evidence emerges if CO daily averages measured on the south and north sides of the street canyon are considered (Table 5-1). On the whole the average during the three-day monitoring campaign was 2.26 mg/m3 on the south side and 2.18 mg/m3 on the north, which are very similar values again. For a better comparison of the CO concentrations measured on the two sides of the street canyon the ratio

$$R = \frac{C_{high}}{C_{low}} \qquad 5.1$$

between the two sides was determined. In Eq. 5.1 C_{high} and C_{low} are respectively the higher and lower CO values measured on the south and north sides of the street canyon at the same hour (it is always $R \geq 1$).

Table 5-1 CO concentrations and ratios between north and south side

	CO daily average		R	
Day	South [mg/m^3]	north [mg/m^3]	daily av. values	Max' hourly values
16	1.35	1.25	1.08	1.52
17	2.35	2.59	1.10	1.95
18	3.09	2.71	1.14	1.59
16-18	2.26	2.18	1.04	1.95

In Figure 5.9 diurnal averages of CO concentrations measured on both sides and CO emission rates in the street canyon are reported. The correlation coefficient between vehicle exhaust emissions and CO concentration is very low (R^2=0.076) that is an indication that meteorological parameters play a dominant role in determining CO concentrations even in a deep street canyon.

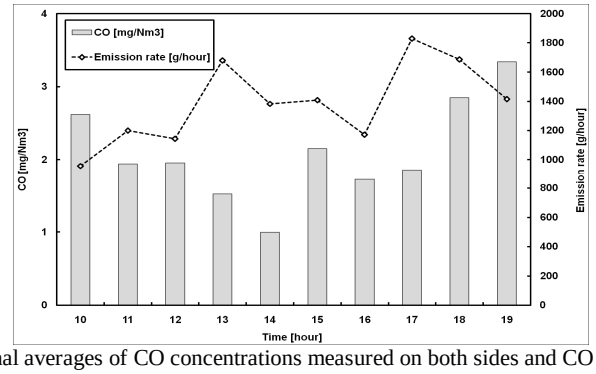

Figure 5.9 diurnal averages of CO concentrations measured on both sides and CO emission rates in the street canyon (from F. Murena at al. 2008)

In Figure 5.10 a wind rose graph with data measured during the three-day monitoring campaign is reported. Data were measured at a meteorological station a few hundred metres from the street canyon. For a better understanding of the correlation between wind direction and values of R, hourly average angles of incidence (α) of the wind with respect to the street axis (70° - 250°) were determined. For wind perpendicular to the street axis α=90°, while for wind parallel to the street axis α=0°. In Figure 5.11 hourly R ratios are reported against the angle of incidence of wind direction α. It can be observed that during the monitoring campaign α ranges between 10° (wind direction mainly parallel to the street axis) and 80° (wind direction mainly perpendicular to the street axis). There is no correlation between the angle of incidence and the ratio R, and even though the wind direction is mainly perpendicular (α> 60°) the value of R is ≅1. Figure 5.11 shows clearly that in our deep street canyon leeward and windward sides do not actually exist.

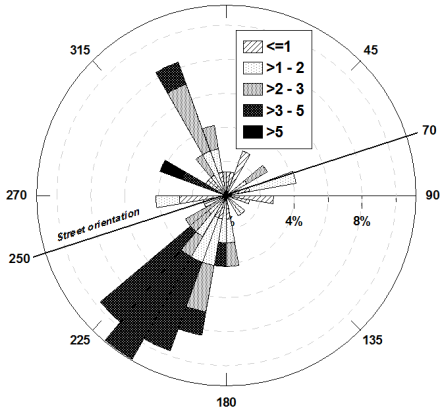

Figure 5.10 wind rose graph with data measured during the three-day monitoring campaign (from F. Murena at al. 2008)

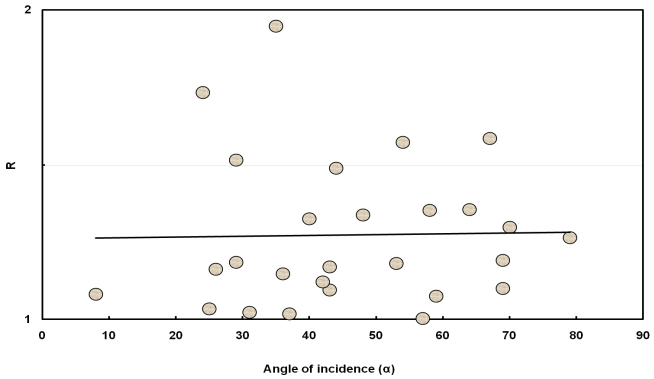

Figure 5.11 hourly R ratios against the angle of incidence of wind direction α (from F. Murena at al. 2008)

6 Input data of the model

Any kind of air quality pollutant model needs input data to give estimation of the pollutant concentration. The number and quality of these data depends on the particular model used. Obviously any model needs, at least, to know the main traffic features, the pollutant emissions amount, the geometrical domain characteristics, the meteorological features and the background pollutant concentration.

The output of any model is strongly affected by the input data quality and accuracy, so, it becomes very important to make a good estimation and make a careful pre-processing of them.

The main traffic features that any model needs to know are the hourly vehicular traffic flow, the mean vehicular fleet composition and the average vehicular velocity. All these information can be obtained by automatic devices placed in the street, manual measurements or extracting data from data bases.

In the present work data on traffic were measured during the monitoring campaigns. In particular the traffic flow was measured from 8 am to 9 pm taking two measurements of 5 minutes each hour. The vehicles were classified into three categories: *"cars"*, *"two wheel vehicles"* and "*other vehicles*" Murena and Favale, 2007; G. Favale, at al (2008) (in preparation), F. Murena, at al (2008).

The COPERT procedure (Ntziachristos and Samaras, 2000) was used to estimate the mean pollutant emission factor for each vehicular class and then to obtain their emission rate [gh^{-1}] in the street canyon. The average vehicular velocity was calculated measuring the time needed by a vehicle to run through the whole street. In particular in via Nardones we found velocity values falling into the range of 20 - 30 km/h. Using the 2004 vehicular fleet data and a velocity value of 20 km/h we can compute these emission factors (Table 6-1):

Table 6-1 Emission factors

Vehicular Class	**Emission Factors (g/km)**
Cars	10.3
Two-wheel Vehicles	17.4
Other Vehicles	5.3

The emission rate for each vehicular class was evaluated as the product of the number of vehicles per hour N_i [h^{-1}], the average emission factor f_i [gkm^{-1}] and the street length L [km]. So the total emission rate was calculated as their sum:

$$E = \sum_{i=1,3} f_i \times N_i \times L \qquad 6.1$$

We have to note that probably the emission rates are over estimated, because this statistical method strongly depends on the fleet composition used and probably the values used report a composition of a vehicular fleet of Naples not applicable at the year 2006.

Obviously any air quality pollution model needs to know the main meteorological features. At least any model has to know the average wind velocity and direction at the roof top level. In this case we used values obtained from a permanent meteorological station situated at the roof top level in the centre of Naples not far from via Nardones.

In order to improve the quality prediction of the model it is very important to consider the influence of the pollution coming into the reference domain from the surrounding areas. It would correspond to concentration at roof top level in upwind direction for wind entering the canyon from the top and to concentration measured in the surrounding upwind streets. It is indicated as background concentration.

Background concentration could be measured using three different approaches: i) by direct measurements of concentration at roof top level and in surrounding streets. This procedure would give the most accurate values, but needs many monitoring devices; ii) by data coming from other air monitoring stations in the urban area; iii), by simulation of pollutant emissions and dispersion in the upwind portion of the urban area. This procedure needs a data base of the emissions in the urban area and a model for the dispersion phenomena on the urban area.

In our case we used the second approach obtaining the background concentration from data coming from permanent air quality monitoring station situated in the urban area of Naples.

7 Two dimensional CFD simulations

Preliminary CFD simulations were carried out on a 2D scenario with the aim to study the effect of the main parameters on the pollution levels in deep street canyon. The results are reported in Murena and Favale (2006). Carbon monoxide (CO) was assumed as model passive pollutant.

The geometry was that of via Nardones (width 5.8 m, height 33. m, aspect ratio H/W≅5.7) assuming that the hypothesis of infinite long canyon would be acceptable. The geometrical domain was mashed using a fine structured grid and steady and unsteady state simulations were carried out.

Steady state simulations were carried out in order to study the velocity field inside the canyon. We set up zero CO emission rate, zero initial and background CO concentrations, a plug-flow velocity inlet condition, i.e. a constant velocity profile on the inflow surface, a symmetry condition on the surface above the roofs and outflow condition on the surface where wind goes out from the computational domain.

Unsteady simulations were carried out assuming at time t=0 a uniform CO concentration in the street canyon and a lower but constant CO concentration in the wind entering the dominion beyond the roof top level ($CO_b = {}^1/_{10}$ or ½ CO(t=0)). In this case the result of the simulation was the reduction rate of CO concentration in the canyon.

The first phenomenon studied was the effect of wind velocity on the flow field generated inside the canyon (range 1-5 m/s). The results obtained by steady state simulations confirm the presence of two vortices as reported in the literature (upper and bottom vortex volumes) (Figure 7.1). The results also show that position and intensity of the vortexes change with changing of wind velocity at roof level, i.e. if the value is very low the intensity of the upper vortex is low and the bottom one does not appear, while increasing the wind velocity the upper vortex becomes stronger, its core goes down in the canyon and the bottom vortex appears.

In order to consider the effect of atmospheric stability several unsteady simulations were carried out by varying the turbulence percentage value (eq 7.1) of wind blowing at roof top level and entering into the computational domain. In the range 10-30% the effect of turbulence percentage on the CO reduction rate is limited and this agrees with Salizzoni, P. at al (2004).

$$I \equiv \frac{u'}{U} \tag{7.1}$$

$$u' \equiv \sqrt{\frac{1}{3}\left(u_x'^2 + u_y'^2 + u_z'^2\right)} \equiv \sqrt{\frac{2}{3}k} \tag{7.2}$$

$$U \equiv \sqrt{\frac{1}{3}\left(U_x^2 + U_y^2 + U_z^2\right)} \tag{7.3}$$

Where u' is the root-mean-square of the turbulent velocity fluctuation and U is the mean velocity Reynolds averaged.

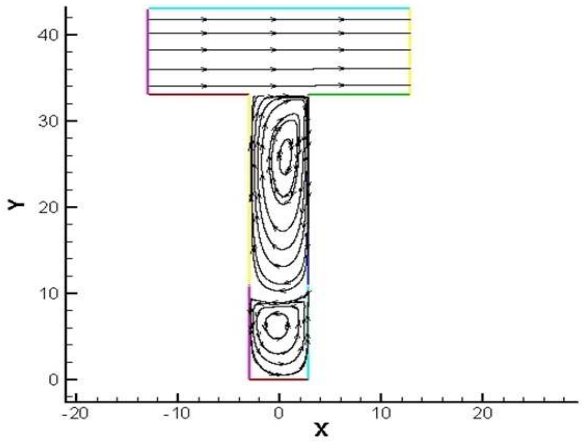

Figure 7.1 Two-dimensional CFD flow field.

Afterward the effect of CO background concentration (C_b) was studied. Simulations were carried out assuming CO at roof top level equal to 0.1 or 0.5 times the concentration at time t=0 in the canyon: i.e.; C_b=0.1÷0.5×CO(0) (Murena and Vorraro 2003). Results reported in (Figure 7.2) show that the CO reduction is strongly dependent from the CO level beyond the roof top level. As matter of fact either in the bottom volume, that is volume that contains the lower vortex, and in the total volume of the canyon, CO concentration increases with increasing of CO background concentration as reported in Figure 7.2.

Vehicles moving in the canyon produce some turbulence which increases mass transfer. The volume where the vehicle induced turbulence is significant (VIT volume) has been identified carrying out some 3D CFD simulations where a parallelepiped volume, representing an idealized car, was hit by a flux of air at 20 km/h in a tunnel having geometrical features like via Nardones. These simulations showed that almost all the increasing of turbulence intensity was contained within a volume ranging from the ground up to 4 metres, and the average turbulence intensity induced by vehicles is about 0.09 kg/(ms^3).

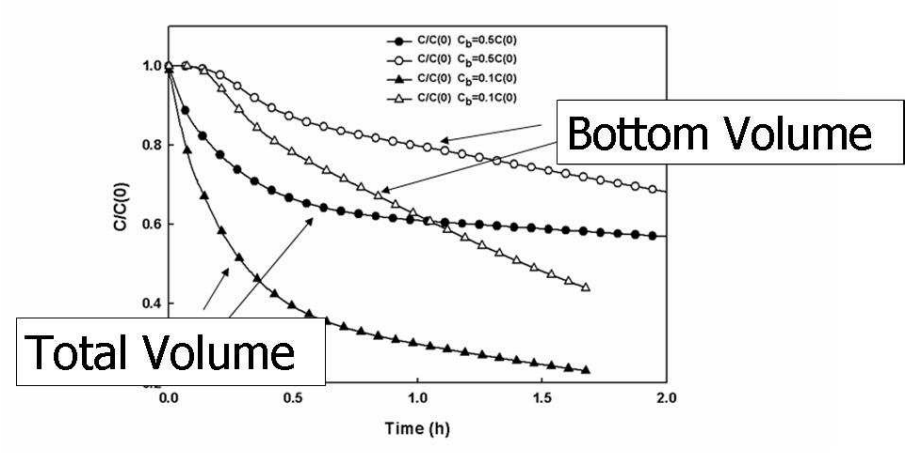

Figure 7.2 Effect of Cb concentration. Full symb.s total volume, empty symb.s bottom volume (Bottom Volume is from ground up to 4 meters, Total Volume is the whole canyon volume)

The effect of vehicle induced turbulence is shown in Figure 7.3 where is reported the CO concentration value in the bottom volume considering two levels of CO background concentration. The figure shows that when *vehicular induced turbulence* is considered CO concentration in the bottom part of the canyon decreases more rapidly.

Finally, the effect of CO emission rate in the street canyon has been considered. Corresponding to highest traffic flow in the canyon a CO production rate of about 10^{-7} kg/sm^3 has been calculated. Simulations were carried out in the range of CO production rate from 10^{-9} to 10^{-6} kg/sm^3. The effect of CO emission on CO vs. time curves is significant. Time necessary to reduce CO concentration level at half the initial value ($CO_{0.5}$) obtained by simulations are reported in (Table 7-1). These values are of the same order of residence time of passive gaseous pollutants in the street (F. Murena and G. Favale, 2006).

Table 7-1 CO half-life time obtained by simulations (wind sped at roof top level = 2m/s)

Turbulence percentage	$C_b/C(0)$	VIT [kg/ms^3]	CO emission rate [kg/m^{3}s]	$CO_{0.5}$ [hr]
10	0	0	0	0.295
20	0	0	0	0.233
30	0	0	0	0.189
20	0.1	0	0	0.233
20	0.5	0	0	0.236
20	0.1	0.09	0	0.263
20	0.5	0.09	0	0.239
20	0.1	0.09	10^{-9}	0.352

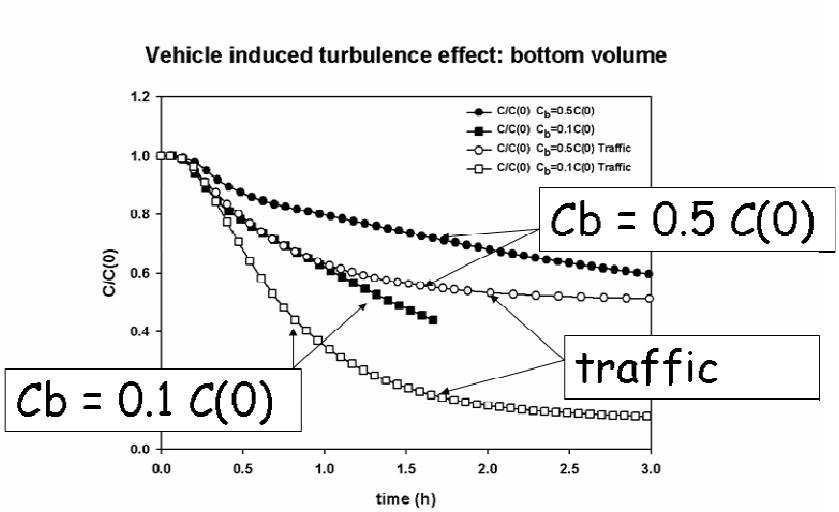

Figure 7.3 Effect of vehicle induced turbulence Empty symbols in presence of VIT (Square symb.s refer to a low background concentration, circles refers to a higher background concentration)

Unfortunately the comparison between data coming from 2D CFD simulations and data coming from monitoring campaigns show that the 2D gives results about ten times higher that those measured. Obviously this over estimation is not acceptable if we want use it as tool for the prediction of the pollutant levels inside a deep street canyon but this model gives us some relevant information about the influence of some parameters, such as VIT intensity and background concentration, on the pollutant level inside the canyon.

8 Three dimensional CFD models

As reported in the previous chapter 7 all the results obtained applying simple a 2D CFD models give us a lot of information about the main feature of the pollutant dispersion mechanism inside the deep street canyon of via Nardones but it gives us over estimation of the pollutant levels. This consideration tells us that we must consider a more realistic model able to describe better the fluid flow inside the canyon taking into account new effects. An improvement is a three dimensional CFD models.

The use of a 3D model instead of a simple 2D allow us to study the case of *parallel* or *near-parallel* flow, that means wind blowing at an angle less than or equal to *30°* to the canyon axis with speed higher than *1.5m/s*, which is obviously not applicable to the 2D model.

The axial velocity component at roof top level causes an axial flux that pushes pollutants, released inside the canyon, out from the domain. The decrease of the pollution level, caused by this phenomenon, is sometimes equal or higher than the decrease caused by the perpendicular velocity component (Savory at al. 2004).

The 3D model also takes into account the presence of the crossing streets which affect the fluid field, especially at pedestrian level, and put in contact via Nardones with the other parallel streets via Chiaia and via De Cesare with a consequently exchange of mass.

The 3D CFD models, like a 2D ones, are able to catch all the main fluid flow features such as the presence of many turbulent vortexes in the street canyon as shown by (Figure 8.1) where the case of wind blowing from a near north direction was considered (angle of incidence between wind and street axis $\alpha = 345^{o}$, wind velocity WV = 1.6 ms^{-1}).

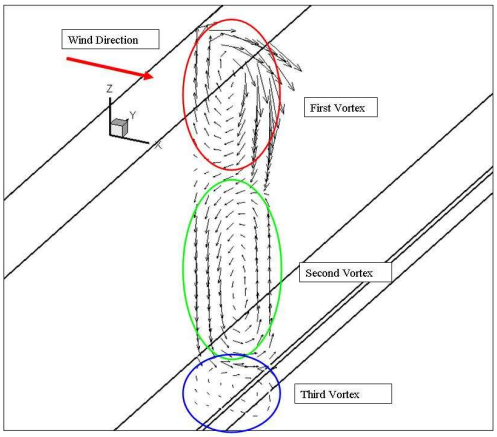

Figure 8.1 Counter rotating vortexes inside a deep street canyon (3D CFD model)

The 3D CFD model also take into account the complex flow patterns generated near the crossing streets (Figure 8.2). All these aspects make the pollutant field, in the domain, really not uniform as we can see in (Figure 8.3). The ability of the 3D model to calculate the complete spatial field of pollutant inside the domain, instead of a mean estimation, is very important because it gives us more information on the sampling points, where measurements were carried out, and on their ability to represent significantly the pollution levels for the whole street canyon.

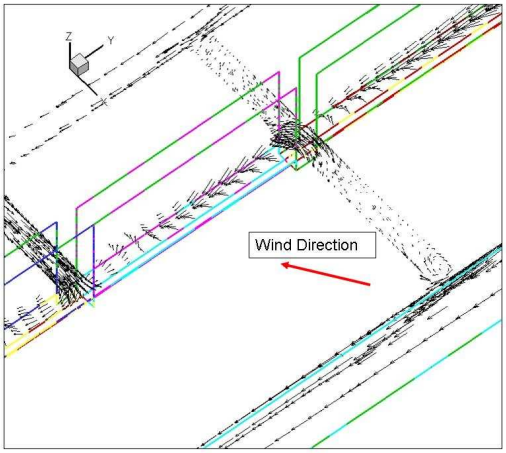

Figure 8.2 Flow pattern inside a deep street canyon (3D CFD model)

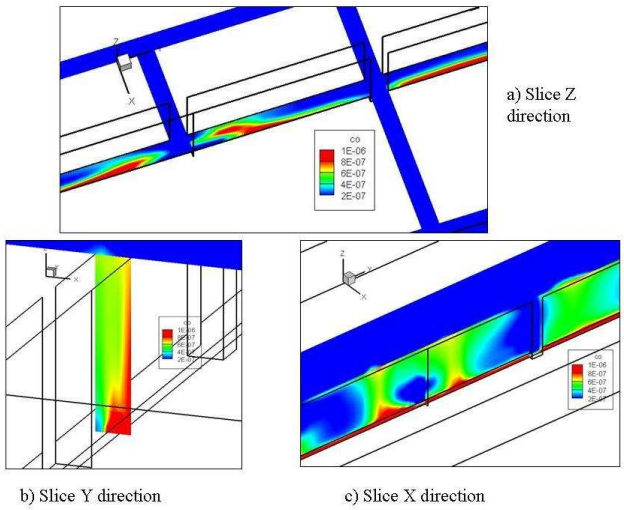

Figure 8.3 CO concentration field inside a deep street canyon (3D CFD model)

8.1 Geometrical models

The 3D geometrical model of the situ of via Nardones was developed taking into account all the surrounding streets of via Nardones, i.e. via De Cesare at north, via Chiaia at south, via Gradoni di Chiaia at west and piazza Trieste e Trento at east. In order to simplify the geometrical features of the model all streets were considered parallel or orthogonal to via Nardones having a constant width and all buildings were considered with the same height.

In order to take in account on the calculus of the pollutant concentration levels inside the situ of Nardones, the effects due to the buildings and streets close to the situ but not considered, different geometrical models were made in two different way.

The first one was obtained excavating the streets inside a solid parallelepiped (Figure 8.4) so the effects of those buildings and streets not considered was simulated only by the surface of the roofs at H = 33.0 meters. In this case we have fixed inflow and outflow surfaces so in order to take in account the variation of the wind direction it was only set up different values of the components x and y of the wind velocity on the inflow surfaces.

This model was called FLUENT-C meaning that it is a complete geometrical model of the situ of via Nardones, anyway a simpler version of it was created not considering the crossing and lateral streets of via Nardones, this last one was called FLUENT-S.

Those two models are very easy to implement but they don't take into account the strong irregularity of the city layer and its influence on the pollutant level estimation.

The second approach that we used was to consider a big fluid parallelepiped where we put in all the buildings (Figure 8.5). The extern buildings were considered much bigger than

in reality in order to make possible the stabilization of the fluid before it is above via Nardones. In this case we considered that the wind always enters into the domain from the same surface so to take into account the variation of the wind direction we must rotate the buildings inside the big parallelepiped like we must do in a wind tunnel. This model was called M2-C being a complete model.

Same preliminary tests were carried out to define the height of the volume beyond the roof top level. The goal is to define a volume as small as possible to reduce computational time but tall enough to contain the turbulent boundary layer that is generated by shear flow on the roofs. Different values were considered and a value of 68.0 meters was adopted. That value guaranties that on the top of the domain the wind flow is almost stable that means that all vertical fluxes are zero.

Also in this case a simpler version of this model, called M2-S, was created; it was obtained not considering the lateral and crossing streets of via Nardones and considering an overall smaller computational domain. This model was used to model data coming from the monitoring campaign of the 16-18 April 2007.

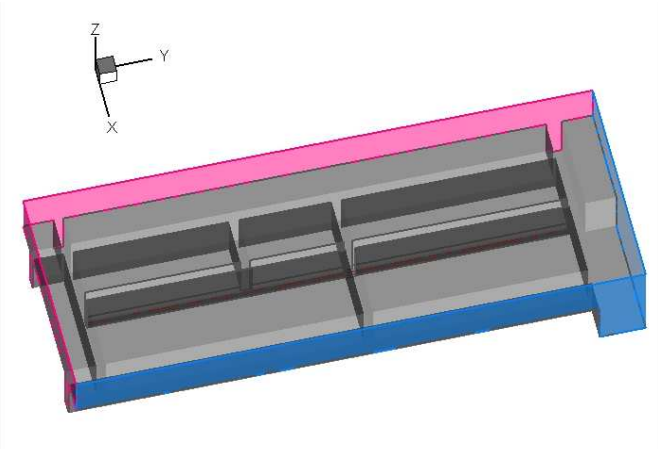

Figure 8.4 Schematic domain of via Nardones (first approach FLUENT-C model)

The pre-processor GAMBIT was used to set up the geometrical model, and then, to mesh it using the large set of functions present in this software.

The volume of our canyon, via Nardones, was divided into three parts in order to distinguish data coming from the east, central and west side of the street, then each part was also split into two volumes, cutting them at 4.0 meters height from the street surface, in order to distinguish data coming from the bottom or the upper part of the street. The value of 4.0 meters was chosen after a CFD simulation, as reported in the chapter 7, where it was considered a parallelepiped representing a car in a tunnel having the same geometrical

features of via Nardones, hit by a wind flow with velocity 20.0 kmh^{-1}. The experiment says that the presence of the car has not effect over 4.0 meters from the ground level.

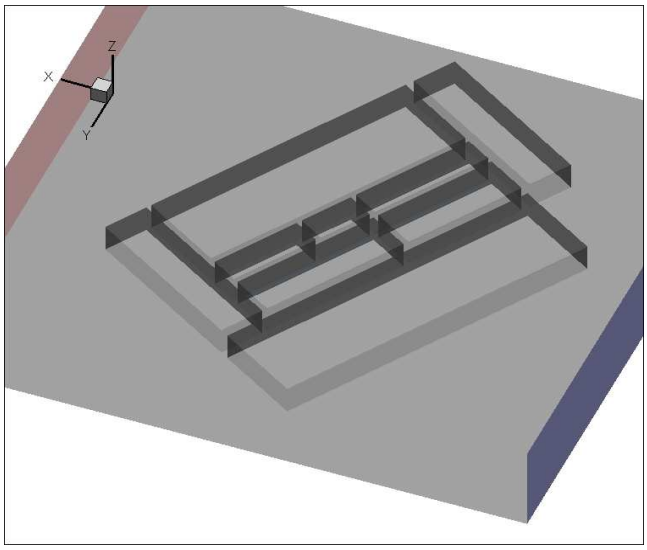

Figure 8.5 Schematic domain of via Nardones (second approach M2-C)

The mesh of the CFD domain was made using two different meshes, the canyon volume was meshed using a uniform conformal grid (Figure 8.6a), while the remaining domain was meshed using a non-uniform method based on tetrahedral volumes (Figure 8.6b). This choice was taken to have a good approximation of the fluid flow in the street canyon keeping the dimension of the model and the computing time reasonably low.

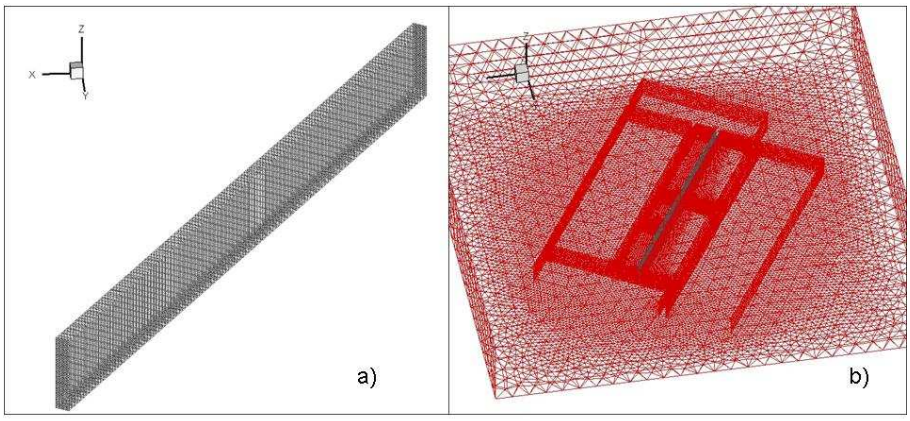

Figure 8.6 a) Mesh of via Nardones, b) mesh of surround area

8.2 Numerical model

As said in chapter 1, the turbulent behaviour of the fluid flow inside the canyon plays a very important role in predicting the pollutants concentration levels, so the choice of a good numerical model, especially referring to the turbulent closure method, is very important.

As we can easily understand between the turbulent models (DNS, LES and RANS) cited in Chapter 3 "Traffic pollution models" the RANS approach allow us to obtain reasonably accurate results limiting, in the same time, the computational effort. Between the available closure methods the RSM model is the more sophisticated and accurate because it define a differential equation for each component of the Reynolds turbulent tensor, but, on the other hand, it is the more onerous, so the complex three dimensional geometry that characterize this model forces us to choice model less sophisticated, such as the κ-ε RNG model.

Another important aspect to take into account is the choice of the numerical algorithms. In order to make a good reconstruction of the spatial and temporal fields of velocity, temperature and concentrations, we adopted a second order implicit method for all time reconstructions, while for spatial reconstructions we used a second order method for pressure and a second order *upwind* method for all the other variables. The coupling between pressure and velocity was made using the SIMPLE algorithm.

Because of the high non linear features of the equations of the model, we have to choice appropriate *under relaxation factors* in order to make the model numerically stable. In this case the lower under relaxation factor was given to the pressure equation (*under relaxation factor* =0.3), then to the momentum equation (*under relaxation factor* =0.7) and to the turbulent kinetic energy and turbulent dissipation rate (*under relaxation factor* =0.8).

Finally the convergence criterion adopted is that the residuals values of any equation must be less than 10^{-6}.

8.3 Boundary conditions

Different kinds of *boundary conditions* were used in this model, all the buildings walls and roofs and the streets pavements were defined as "*wall boundary*" i.e. setting, on these surfaces, zero shear and impermeability conditions.

All the outflow surfaces were defined as "*outflow boundary*" that means that the outgoing flow is build using a zero diffusion flux condition for all the variables with an overall mass balance correction.

On the other hand the surfaces from which flux comes into the domain are defined as "*velocity inlet boundary*" that means to set the profile of all the quantity coming into the domain such as velocity components, temperature, turbulence and pollutants concentration. In order to represent in a more realistic way the flux incoming we used three functions to describe the velocity and turbulent profiles:

$$v = v_r \left(\frac{z}{z_r} \right)^m \quad 8.1$$

$$k = \beta v^2 \quad 8.2$$

$$\varepsilon = C_\mu^{3/4} \left(\frac{k}{k_v z} \right)^{3/2} \quad 8.3$$

Where: m=0.28; β=0.03; C_μ=0.09; κ_v (Von Karman constant) = 0.41 and v_r is a reference velocity measured at a reference height.

The exponential profile for horizontal wind velocity (eq.8.1) is a common choice for describing a fully developed boundary layer (e.g., Meroney et al., 1996). The power m is typically less than or equal to unity, depending on surface roughness and atmospheric stability. Comparison of observed wind-speed profiles from different sites and different stability classes indicates that m increases with increasing surface roughness and with increasing stability. Under near-neutral conditions, m ranges from 0.15 for very low surface roughness to 0.4 for well-developed urban areas (Pal Arya, 1999). For a surface roughness of 3.0 m corresponding to central areas of cities, m ranges from 0.27 (corresponding to Pasquill class A, i.e. very unstable) to 0.69 (corresponding to class F, i.e. very stable). The value of 0.28 assumed for m in this study corresponds to Pasquill class B, which is typical of the atmospheric stability conditions occurring in Naples.

Wind turbulent intensity above roofs can vary widely depending on the atmospheric stability and roof surface roughness. It can affect the pollutant dispersion inside a street canyon. Kim and Baik (2003) studied this effect on a 2D street canyon model with AR=1 changing the turbulent kinetic energy (TKE) of wind using values of β in the range 10^{-3}-10^{-1} and assuming that inflow turbulence energy is relatively weak for β up to 0.045 and relatively strong when β > 0.045. Sini et al. (1996) modelled a street canyon with H/W from 0.1 to 3 assuming a low turbulence intensity β =3×10^{-3}). Turbulent kinetic energy is actually subject to daytime diurnal variation in the convective boundary layer. It typically reaches a maximum value in afternoon depending on the atmospheric stability.

In our simulations we assumed β=3×10^{-2} being constant with time. For simplicity, we do not take into account the diurnal variation of TKE, although it could have an effect on diurnal variation of CO concentrations within the street canyon (Kim and Baik, 2003).

In order to simulate the input of CO from vehicles in the street canyon we defined an inflow surface, having width of 2.0 meters and length 315.0 meters, at the centre of the road surface of via Nardones from which a mixture of air and pollutant comes into the domain with a constant velocity of $0.1 ms^{-1}$ in order to model the pollutant rise due to the buoyancy effect.

Finally, in order to take into account the vehicle induced turbulence (VIT) effects, which are significant when the wind velocity is small (WV < 1.5 m/s at roof top level) (Solazzo at al., 2007), was introduced in the bottom part of the modelled canyon, from the ground up to 4.0 meters height, a TKE production per unit length P_T (eq. 2.1) calculated

assuming a constant average vehicular velocity of $v_v = 20.0$ km h^{-1} , a vehicular frontal area of $A_T = 3.2$ m^2 and a drag coefficient of $C_{DT} = 0.3$.

9 Application of the three dimensional CFD model

The hardware used to carry out three CFD simulations is a workstation with two CPU AMD Opteron, despite the high performance of this machine the computational time needed for a 3D CFD simulation is quite large. Typically to simulate a physical time of one hour we need from two to four hour of CPU computation depending on the convergence criterion and the equation stiffness.

9.1 Influence of the siding streets

In order to understand how the presence of siding streets influences the pollutant dispersion in our deep street canyon, via Nardones, different simulations were carried out comparing the results of the 3D CFD model described in chapter 8.1 and indicated as FLUENT-C with its simplified version FLUENT-S obtained eliminating the two siding streets, the meteorological and emission data used are that reported in chapter 9.3 while the background concentration used is that obtained from the air quality monitoring stations (Murena and Favale, 2007 b).

Results obtained from both models show, as reported in Figure 9.1, that both are able to predict pollutant concentration levels of the same order of measured values, with a significant improve compared to the 2D model. This result show that the axial wind velocity has a strong effect on the concentration of pollutant inside a street canyon

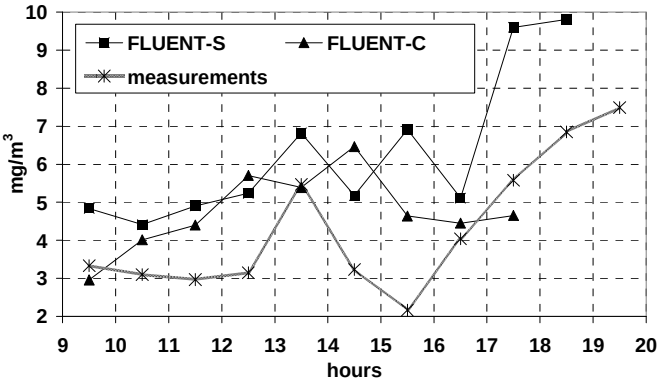

Figure 9.1 Hourly average values of CO concentration measured by CO analyzer (x) and evaluated by simplified model (box) and complete model (triangle)

Analyzing Figure 9.1, it seems that the simplified model can better follow the hourly variation of CO measured data than the complete model. As a matter of fact the simplified model curve significantly differs from measured one only in a single point i.e. between 15 and 16 hours, while the complete model curve differs between 13 and 14 hours and from 16 to 18 hours. On the other hand complete model provides hourly average values lower than simplified model and closer to measured values.

Figure 9.1 shows that both models generally over estimate data measured during the monitoring campaign of 15th June 2006. Even though they represent an improvement compared to the 2D CFD model deeper analysis are necessary to improve the CFD model.

Comparing the mean square error values of the two models, as reported in Table 9-1, we can see that the complete model has a better correlation with measured values.

Table 9-1 Mean square errors between measurements and model values

	FLUENT-S	**FLUENT-C**
$\frac{1}{N}\sum_{i}^{N} e_i^2$	6,62	3.01

9.2 Influence of the background concentration

Another important aspect that we have to investigate, to improve knowledge on dispersion mechanisms occurring in deep street canyons, is the influence of background concentration. In order to make this we used the 3D CFD model FLUENT-C to make two simulations, the fist assuming as background concentration that measured at 25 meters, in order to consider a background concentration probably higher than the actual one but having a distribution with time close to that of actual background concentration, the second assuming background concentration =0. Figure 9.2 clearly shows how the pollutant background concentration plays a significant role in the pollutant concentration level in the deep street canyon and that is in agreement with results obtained by 2D CFD code as reported in chapter 7. When Cb is assumed = to C25m the concentration at bottom level is higher than that measured while if it is assumed Cb=0 the modelled values are lower than the experimental ones. The ratio between the two modelled curves is about 3-4. This means that the quality of the calculation of concentration inside the canyon depends strongly on the quality of the estimation of the background concentration. Finally we can note that this aspect is consistent with the observation, reported in chapter 5, that during night hours sometimes the concentration at top level is higher than at bottom level, probably because the emission rate is almost zero while background concentration is not negligible so pollutant comes into the domain from the top of the canyon and the vertical gradient of concentration is opposite from the usually.

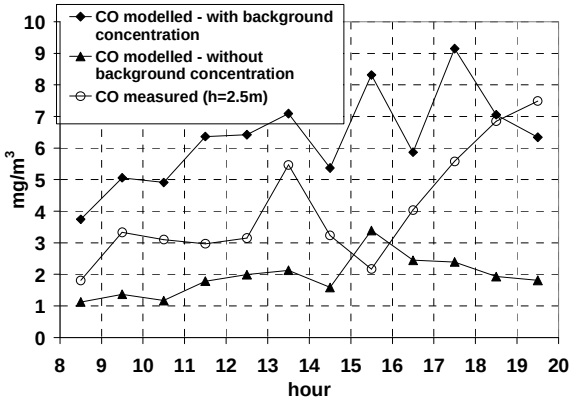

Figure 9.2 Comparison between CFD simulations and monitoring data influence of background concentration (from G. Favale at al. 2007)

Our model is also able to predict with good approximation the pollutant concentration in the upper volume of the canyon as reported in Figure 9.3 where the average CO concentration calculated in the central bottom and upper volumes are compared with measured values at two sampling points, the first at 2.5 meters and the second at 25 meters from the ground level.

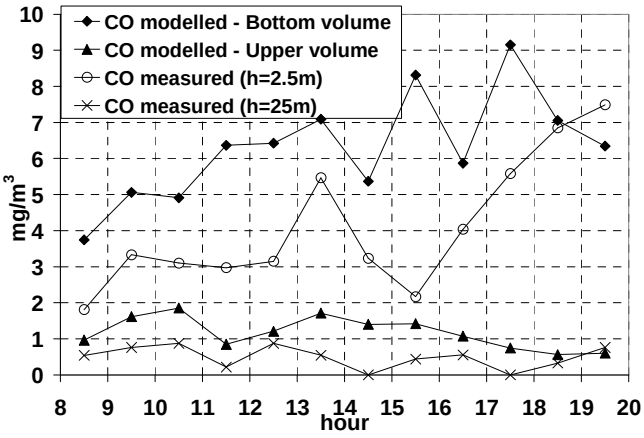

Figure 9.3 Comparison between CFD simulations and monitoring data at different height (from G. Favale at al. 2007)

9.3 Effect of Vehicle Induced Turbulence (VIT)

To investigate on the effect of VIT simulations of data collected during the monitoring campaign carried out from 14 to 20 June 2006 (Murena and Favale, 2007 a) were carried out. The day selected was the 15th June 2006.

During this day we collected traffic data from 9 am to 8 pm, so we can calculate the traffic emission rate only in this range and, consequently, compare computed and measured data only in this range (Figure 9.4).

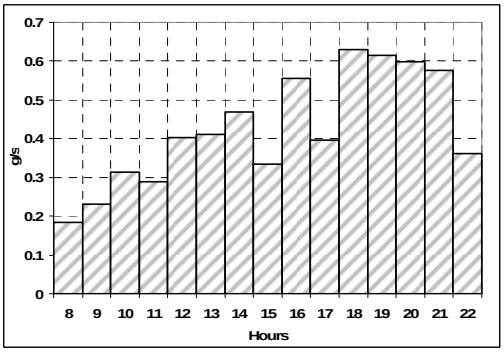

Figure 9.4 vehicular emission rate of CO (15 June 2006)

The input meteorological field at the roof top level was obtained hourly averaging the wind velocity and direction values obtained by a permanent meteorological station as reported in (Figure 9.5).

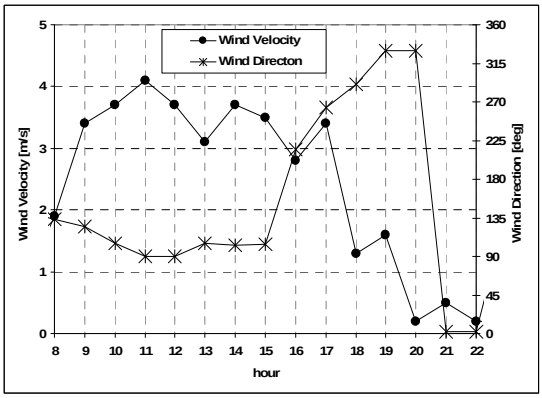

Figure 9.5 Hourly average values of wind direction (star) and wind velocity (circle) (15 June 2006)

Results obtained applying the model M2-C defined in chapter 8.1 are reported in Figure 9.7, a comparison between CO concentrations measured at 2.5 m (south side) and modelled with CFD (south side) (Figure 9.6) is reported. Simulation results cover the period from 8:00 to 22:00, because CO emission rates in the street canyon were unknown from 0:00 to 8:00 and from 22:00 to 24:00 (traffic flow was not measured during those hours). Experimental data reported in Figure 9.7 were obtained hourly averaging data measured every minute at the sampling point and error bars were calculated considering a confidence interval CI = 99%.

Figure 9.7 shows a good correlation between experimental and CFD modelled concentration of CO apart from the value at 16:00. If this value is not considered the correlation factor is R=0.95 (Figure 9.9(a)). However, CFD simulations generally overestimate the actual CO concentrations.

Figure 9.8, where concentration at north and south side obtained from CFD simulation were reported, also shows that CO concentration modelled at the south and the north sides of the street are very similar if VIT effect is considered. This finding is in agreement with CO concentrations measured on both the sides of the same street canyon during the intensive monitoring campaign (Murena et al., 2008). If VIT is not taken into account in the CFD simulations, the CO concentration on the two sides are slightly different (Figure 9.7(b)) and correlation with measurements decreases R=0.87 (Figure 9.9 (b)).

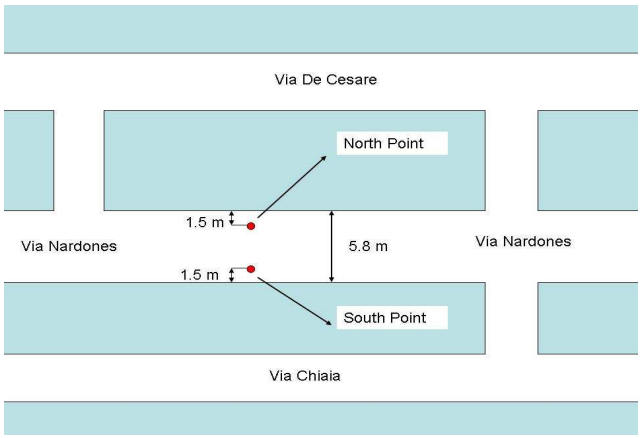

Figure 9.6

In order to better investigate on the influence of the wind direction and intensity and vehicle induced turbulence on the CO concentration at the south and north side of the street canyon CFD simulations were carried out using a simplified version of the model of via Nardones defined M2-S as reported in chapter 8.1. Six wind directions were selected on the basis of the more frequent directions as reported in wind rose graph of Figure 5.10. Wind

direction was assumed in all the case as 2 ms^{-1} at the reference height of 50 m from the ground level and to take in account the effects of mechanical turbulence generated by the traffic within the canyon a Turbulence Kinetic Energy production in the bottom part of via Nardones was introduced using the function in eq. (2.1)

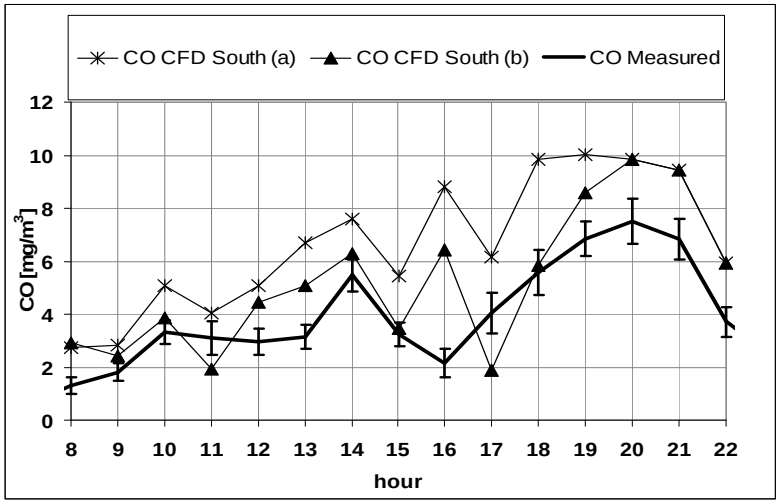

Figure 9.7 Comparison of CO concentration measured at z=2.5 m and CFD simulation - 15 June. Note: Case (a) with Vehicle Induced Turbulence, Case (b) without.

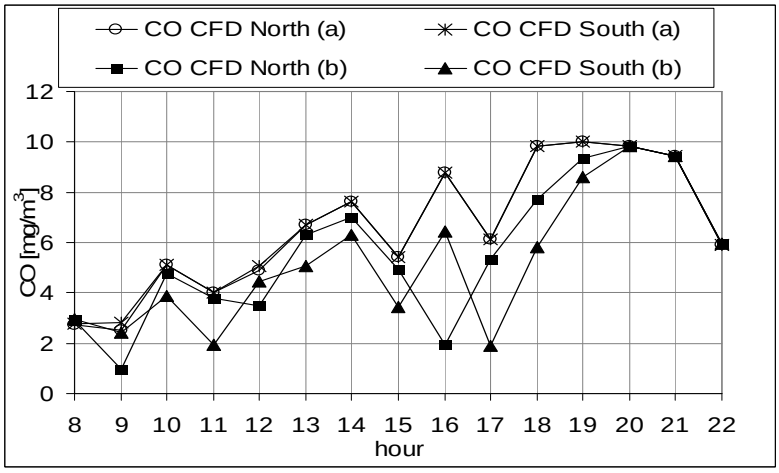

Figure 9.8 CFD simulation - 15 June. Note: Case (a) with Vehicle Induced Turbulence (VIT), Case (b) without VIT.

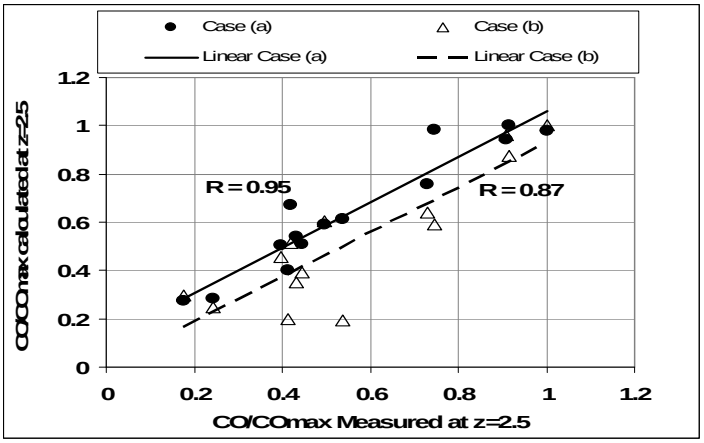

Figure 9.9 Correlation between CO concentration measured at z=2.5 and CFD model results - 15 June Note: Case (a) with Vehicle Induced Turbulence, Case (b) without VIT.

The results of the CFD simulation are reported in Figure 9.10 plotting the ratio R (eq. 5.1) calculated by FLUENT in correspondence of the sampling points (Figure 5.6) versus wind velocity direction for both cases with VIT introduction and without VIT.

Figure 9.10 shows that the difference between CO concentration at south and north side of the canyon is higher when wind at roof top level is almost orthogonal either we consider the VIT effect or not. At mean time Figure 9.10 shows that vehicle induced turbulence plays a significant role in determining the CO concentration at the two sides of the street. The introduction VIT makes the ratio R very close to one which means that concentration of CO on the south and north side of the canyon are almost equal because of the mixing generated by the traffic.

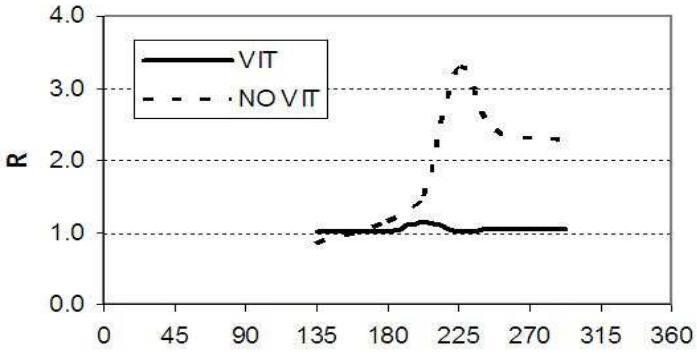

Figure 9.10 values of ratio R calculated by FLUENT in correspondence of the sampling points (Figure 5.6) (from F. Murena at al. 2008).

10 Application of a parametric model (OSPM) to the deep canyon of via Nardones

As reported in the chapter 2 many parametric models (STREET, CPBM, OSPM) were created in order to calculate the pollution levels in street canyons. These models are of simple use and could be a powerful tool for public administration in managing air quality in urban areas. However, they were developed and tested for *regular street canyons* (i.e. AR ≈ 1) (J. Kukkonen at al. 2001) and not for *deep street canyon* (i.e. AR > 1).

We intend to apply the OSPM model at our street canyon and to compare the results obtained with experimental data and results of CFD simulations.

Particularly we chose the WinOSPM which is an *Operation Street Pollution Model* able to predict the concentration level of inert (e.g. CO) and fast reacting (e.g. NO_2) pollutants in urban street canyon type geometries. The WinOSPM is widely used as tool for fast calculation of pollutant levels in cities by many national organizations, for example it is used for surveillance of air pollution from traffic in Danish cities and it is also used for many special air pollution studies. (S. Vardoulakis at al. 2007, A. Ziv at al. 2002)

A first comparison between the CFD and WinOSPM model were obtained comparing CO vertical profile (*north* and *south* side of the street Figure 9.6) calculated by the two models on a reference case where the background concentration and the *vehicular induced turbulence* (VIT) were not considered. Results are reported in Figure 10.1and Figure 10.2 (as reported by Favale et al. 2007).

In Figure 10.1 and Figure 10.2 are also reported the concentrations measured at 2.5 meters obtained subtracting the background concentration, as we can see both model are able to predict concentrations very close to the measured ones.

Both models predict similar CO concentration levels and have a good agreement near the roofs, but at street level there are some differences. As shown by Figure 10.1 c and d, when the wind direction is almost parallel to the road axis, both models predict fast decrease of CO concentration with height but the CFD model, also predict different CO profiles in north and south side of the road. When the velocity direction is not parallel to the road axis the WinOSPM model predict a constant concentration of CO inside the canyon, while the CFD model is already able to predict a non uniform distribution, as reported in Figure 10.1 a, b and Figure 10.2 a, b, d. Probably, in the WinOSPM model, there is this behaviour because of the extension of the recirculation zone to the whole canyon and the influence of the direct contribution of the vehicular plum is only limited to the bottom part of the canyon. The CFD model, instead, has the ability to predict inside the canyon the presence of many turbulent vortexes which cause a decrease of the dilution along the height.

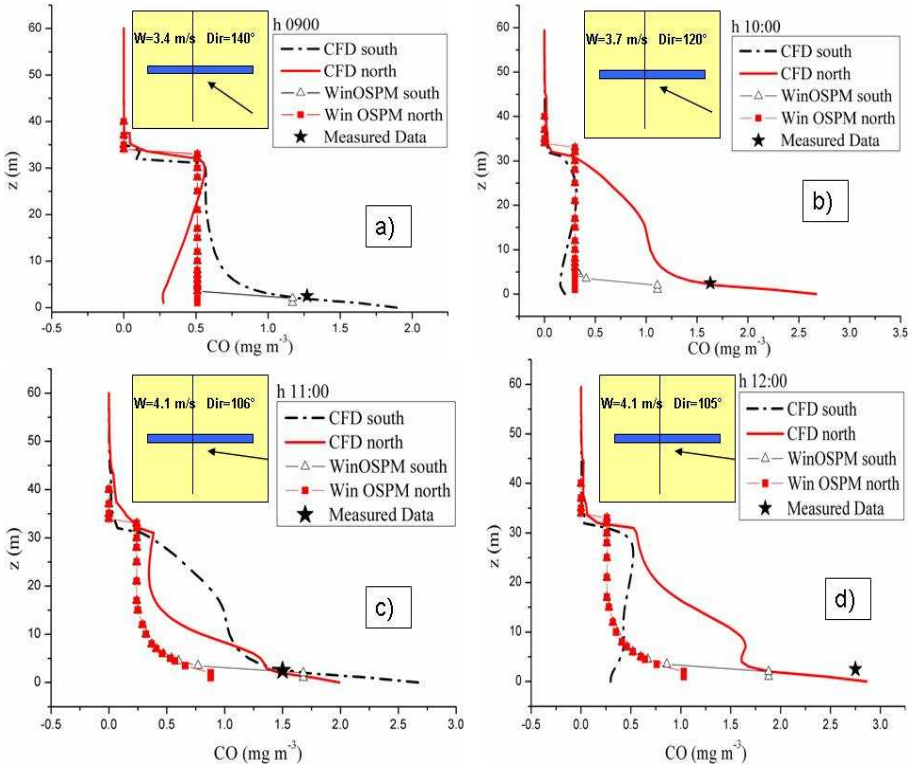

Figure 10.1 (as reported by Favele et al. 2007) Vertical CO concentration computer with WinOSPM and CFD on the North and South side of the canyon (15 June 2006, hours from 9 to 12)

As we can see in Figure 10.1 a) and Figure 10.2 d) when the wind is not parallel to the street axis the concentration estimate by CFD model at North side are close to that estimate by the WinOSPM model for the South side. That probably is due to the presence, inside the canyon, of multiple counter-rotating vortex which the CFD model is able to predict.

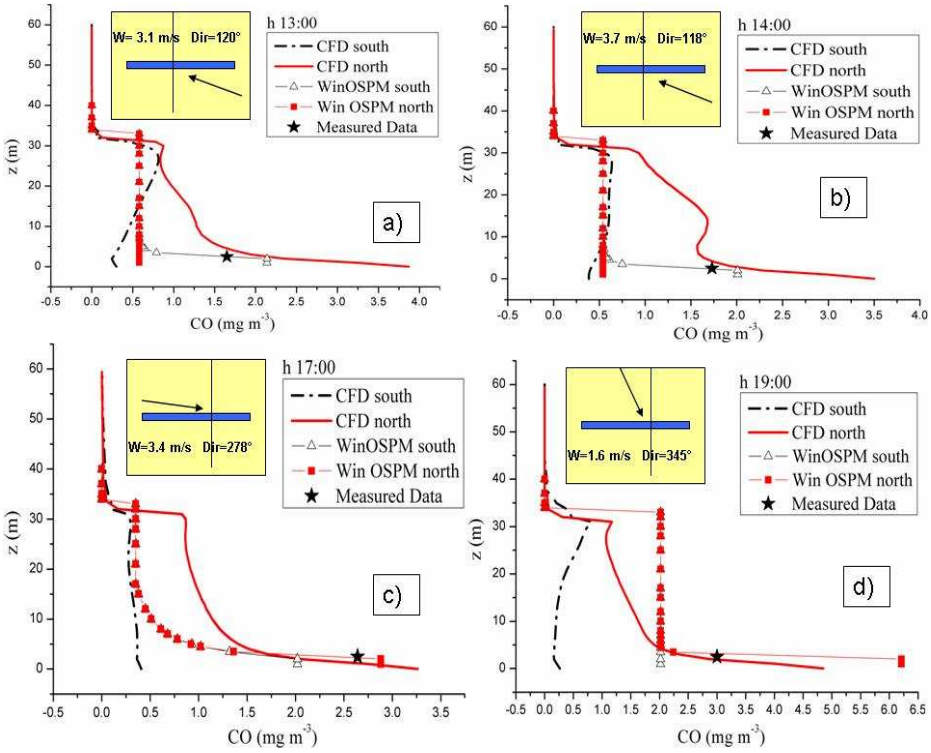

Figure 10.2 (as reported by Favele et al. 2007) Vertical CO concentration computer with WinOSPM and CFD on the North and South side of the canyon (15 June 2006, hours from 13 to 19)

Another comparison is reported in Figure 10.3. This figure reports the comparison between CO concentrations measured at height 2.5 meters during the monitoring campaign of 15th June 2006 and those calculated using the WinOSPM model.

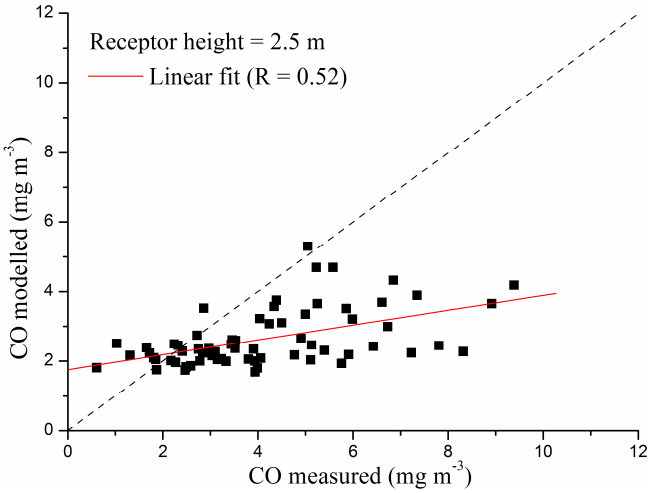

Figure 10.3 Measured vs. modelled CO concentration at receptor location (z1 = 2.5 m) by using WinOSPM. Linear fit and correlation coefficients (R) (from Favale et al. 2007).

The correlation between data is poor (R=0.52). In same cases the model overestimates the CO concentration (especially at low concentration levels) in other case (higher CO levels) the model underestimates the CO concentration.

The poor correlation obtained is not surprising because this model was developed for regular street canyons. A possible explanation of the poor correlation of data in Fig. 10.1 is the erroneous modelling of the flow field in the canyon performed by WinOSPM model. The hypothesis of logarithmic reduction of the wind velocity from the roof to the ground level (eq. 3.23) could be not applicable in the case of deep street canyons. For this reason the flow field inside the canyon will be deeply discussed in the next chapter

11 Flow field within the canyon

The flow field determined by roof top level wind within a street canyon may be quite complex depending on the geometry of the canyon and the wind direction. The simplest case is the flow developing within that of an idealised street canyon, consisting of a parallelepiped 3D cavity of infinite length open at the top, when the wind direction is perpendicular to the street axis. This is also the most frequently studied case, because it corresponds to the worst pollution scenario. The wind blowing at roof top level generates a vortex-like flow inside the canyon. The dispersion of pollutants released at ground level from vehicle exhausts depends strongly from the flow field (both direction and speed) generated inside the canyon and from other phenomena like vehicle induced turbulence (Di Sabatino et al., 2003; Kastner-Klein et al., 2003; Solazzo et al., 2008) or thermal effects (Sini et al. 1996). On the basis of the simple scheme of one vortex like flow, some parametric (operational) models have been developed, where the wind profile inside the canyon is calculated through simple relationships (Hotckiss and Harlow 1973), or assuming a logarithmic reduction of the wind speed within the cavity (OSPM).

In Figure 11.1, the flow field in a section of via Nardones corresponding to the sampling points is shown. This figure shows the streamlines calculated on two planes: perpendicular and parallel to the street axis. Six different hours on 15th June are considered, characterized by different wind velocity intensity and direction.

Figure 11.1a and Figure 11.1b represent cases where wind blows from south-east direction (133° at 8 a.m. and 128° at 9 a.m.). In this case both wind components parallel and orthogonal to the street axis are not negligible. In fact, the angle of incidence is $\alpha = 63°$ at 8 a.m. and $\alpha = 58°$ at 9 a.m.. Figure 11.1a and Figure 11.1b show the presence of a vortex in the upper part of the canyon which sinks into the canyon on the plane vertical to the street axis. Its intensity is higher at 9:00 corresponding to the higher wind velocity at roof-top level (3.4 m s^{-1}) compared to the wind velocity at 8:00 (1.9 m s^{-1}). The flow field on the plane parallel to the street axis show the presence of a vortex generated by the flux coming from the nearest surrounding streets. In these cases, this flux affects the air flow inside the canyon more than the parallel roof-top wind velocity component.

Figure 11.1c and Figure 11.1d show cases where wind velocity is almost parallel to the street axis. Figure 11.1c corresponds to 11 a.m. with wind direction WD = 90°; angle of incidence $\alpha = 20°$ and wind velocity WV = 4.1 m s^{-1}. Figure 11.1d corresponds to 12 a.m. with wind direction WD = 90°; angle of incidence $\alpha = 20°$ and wind velocity WV = 3.7 m s-1. Both cases are characterized by an axial vortex clearly generated by the axial wind velocity component, whose position and intensity depend on the wind velocity magnitude. When velocity is high as at 11:00, the vortex on the plane vertical to the street axis disappears.

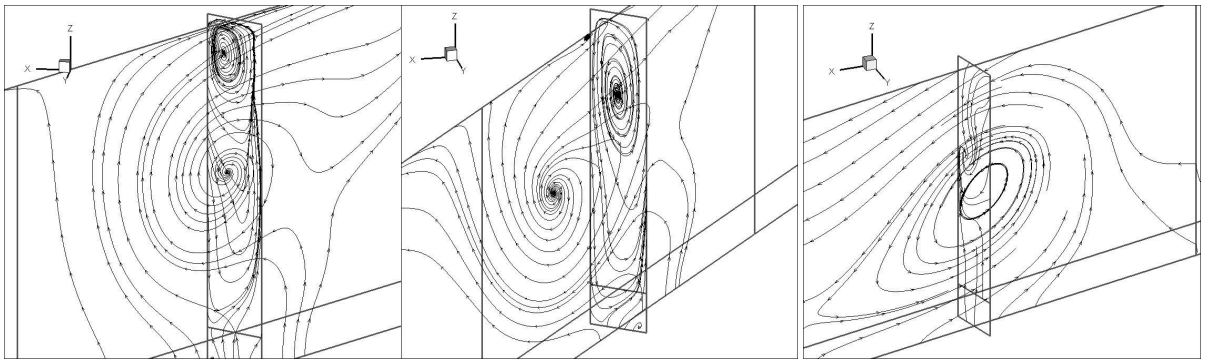

a)hr=8, WD=133°,WV=1.9m/s b)hr=9, WD=128°,WV=3.4m/s c)hr=11, WD=90°,WV=4,1m/s

d)hr=12, WD=90°,WV=3.7m/s e)hr=16, WD=220°,WV=2.8m/s f)hr=19, WD=330°,WV=1,6m/s

Figure 11.1 –Flow field within the street canyon in different wind direction (represented by the x axis) and intensity conditions. Section is in correspondence of the sampling point (Figure 5.1)

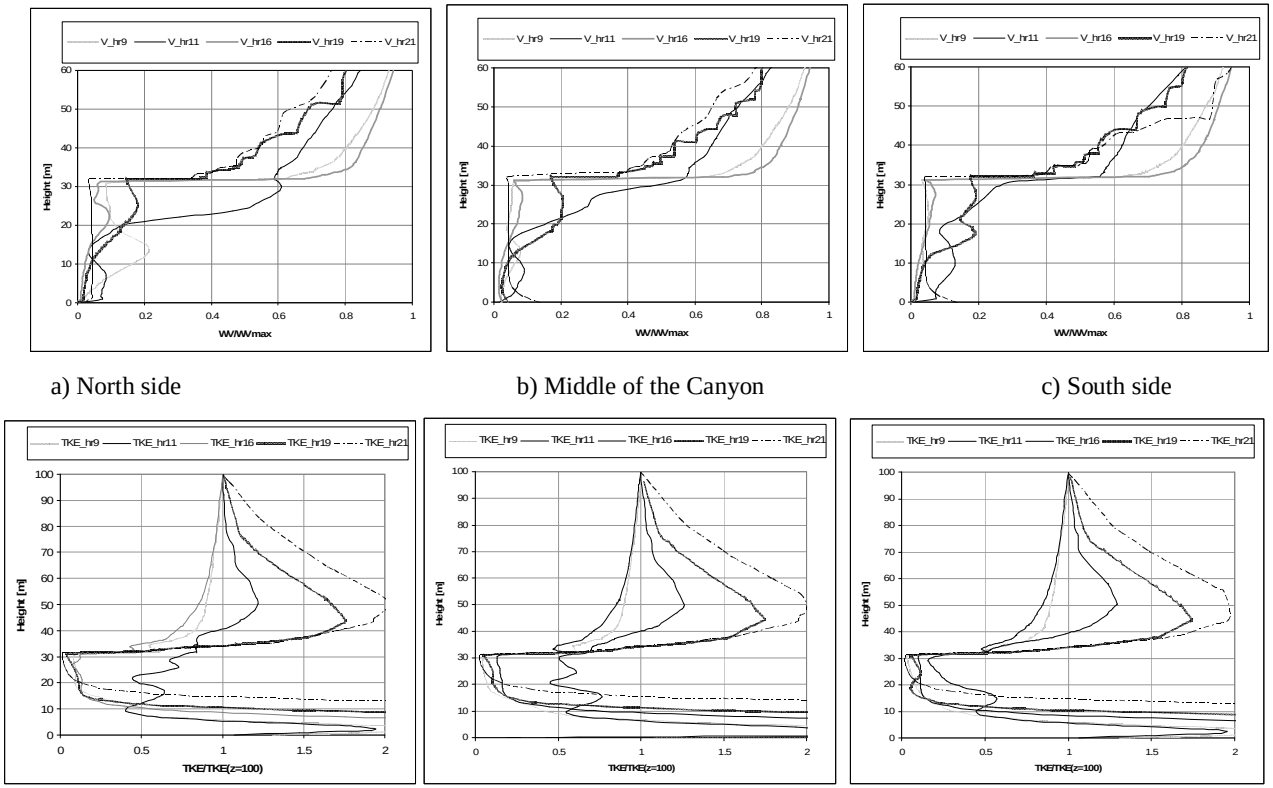

a) North side b) Middle of the Canyon c) South side

Figure 11.2 CFD profiles of WV/WVmax and TKE/TKE(z=100m) in correspondence of the sampling section

Figure 11.1e shows the flow field at 16:00 with wind direction WD = 220°; angle of incidence $\alpha = 30°$ and wind velocity WV = 2.8 m s^{-1}. In this case, the wind direction is from south-west, the flow field is similar to cases of Figure 11.1a and Figure 11.1b but now the influence of surrounding streets is less pronounced.

Figure 11.1f represents a case of northern wind direction (19:00, wind direction WD = 330°; angle of incidence $\alpha = 80°$, and wind velocity WV = 1.6 m s^{-1}). In this case the vertical wind component is predominant and the air flow inside the canyon is characterized by a strong vortex on the perpendicular plane.

In Figure 11.2, the vertical wind profile evaluated at 1 m distance from north wall of the canyon (north side), in the middle of the canyon, and at 1 m from the south wall (south side) is reported at 9:00, 11:00, 16:00, 19:00, and 21:00 as v/vmax. A sharp decrease in wind speed near the top of the canyon at height of approximately H = 33.0 m. Inside the street canyon, the wind velocity decreases but not in a regular way reflecting the complex flow fields showed in Figure 11.1. At 9:00, the velocity pattern at the north side is strongly influenced by the stream coming from the near intersecting street that accelerates the local air flow. At 11:00, when the wind is almost parallel to the street axis, the wind velocity within the canyon decreases less steeply with height because the wind meets less obstacles and the wind velocity pattern follow the undisturbed profile. At 19:00, the presence of a strong vortex increases the wind velocity in the upper part of the canyon and, since this vortex has its centre near the south face, the velocity is higher in that zone. At 21:00, the velocity intensity is very low. It should be noted that the CO source as an inflow with a constant vertical velocity of 0.1m/s at the road surface, therefore the velocity at z = 0 is not zero.

Figure 11.2d, Figure 11.2e and Figure 11.2f show the turbulent kinetic energy profiles normalised with their values at 100 m height (TKE/TKE100). The TKE profiles have a maximum in the shear region above the roof level (not always!) and in the bottom region of the canyon due to the vehicle induced turbulence.

It was observed that all profiles have a similar shape except for the profile at 11:00 when the wind direction is almost parallel to the street axis and the TKE decreases less rapidly compared to the other cases. At 11:00, the irregular pattern within the canyon is due to the presence of a strong vortex in the axial plane due to the axial wind velocity component.

The TKE in the upper part of the canyon increases from the leeward to the windward side at 9:00, when the wind blows from a south-east direction the TKE at the south side is lower than at north side and, in the contrary, at 19:00 when the wind blows from a north-west direction the TKE increases from north to south side.

12 WinOSPM modification

In order to adapt the WinOSPM model to the deep street canyon problem some changes to the function (eq. 3.23) that simulates the wind profile within the canyon were made.

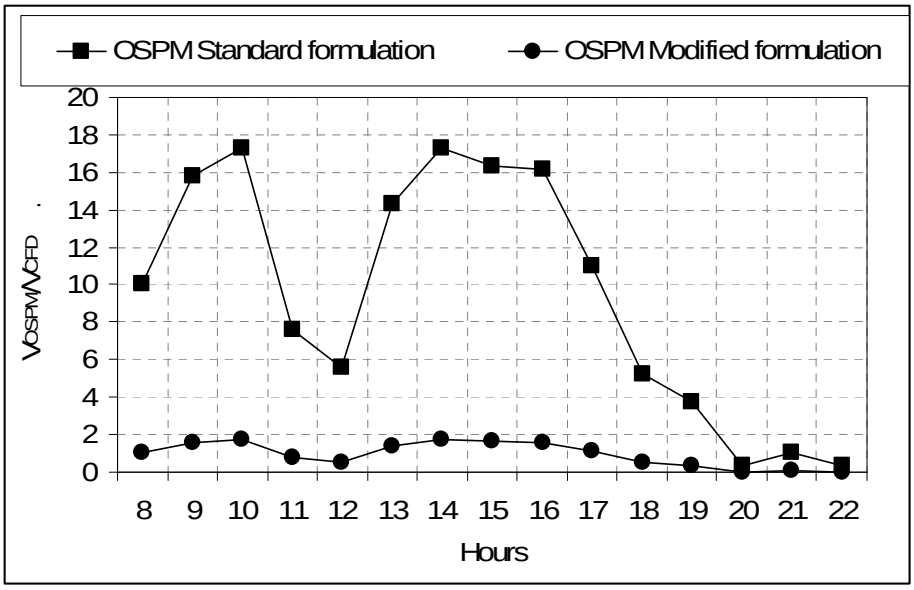

Figure 12.1 Comparison of wind velocity profiles modelled by CFD and OSPM (from Favale at al. 2008)

Figure 12.1, where the ratio v_{OSPM}/v_{CFD} evaluated at the centre of the canyon close to the ground is reported, shows that wind velocity reduction applied by WinOSPM inside the canyon is not sufficient for a deep street canyon such as via Nardones. In fact, street-level wind velocity simulated by WinOSPM is on average 10 times higher than the values produced with the CFD code. Only between 20:00 - 22:00, the two models are in good agreement. It is evident that the logarithmic function implemented in WinOSPM is not able to simulate the flow field in a deep street canyon. This is because WinOSPM model was originally developed for regular street canyons with AR ≈ 1 (Berkowicz, 2000). The unrealistic representation of the flow field within the deep street canyon by WinOSPM may

be a reason of the bad capacity of the model to reproduce the observed CO concentrations (Figure 10.3).

By applying a further reduction of the street level wind speed by an empirical factor of 10 within the model, the ratio of v_{OSPM} to v_{CFD} at street level comes closer to the value of 1 (Figure 10.3).

Results in terms of correlation between CO concentrations modelled by WinOSPM and experimental data are remarkably improved after applying the empirical wind speed reduction factor in WinOSPM as shown in Figure 12.2.

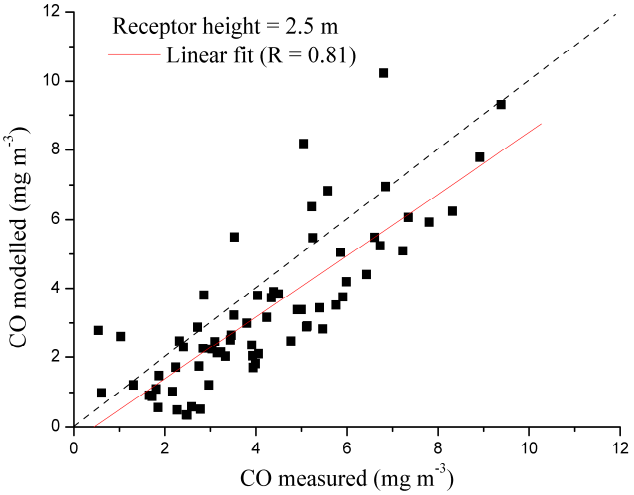

Figure 12.2 Measured vs. modelled CO concentration at receptor location (z1 = 2.5 m) by using a reduction factor for the wind speed 10 times higher than the default value set in WinOSPM. Linear fit and correlation coefficients (R) (from Favale et al. 2008).

13 Conclusions

In this thesis was studied the mechanism of dispersion of passive pollutants released from vehicles in narrow streets that we referred as *deep street canyons*. We chose this kind of streets because of their diffusion in the historical centres of many Mediterranean cities like Naples. Those streets are sometimes characterized by bad air quality with high pollution level because of their low ventilation.

This phenomenon is very difficult to study because it depends on many variables such as geometry of the street, meteorological and traffic conditions and it is characterized by different spatial and temporal scales.

Monitoring campaigns were carried out in order to analyze the pollution field and its dynamic inside a deep street canyon. Results show that in deep street canyons high level of vehicle pollutants could be reached, especially at pedestrian level, even though urban monitoring stations measure lower values.

In order to better understand the mechanism of dispersion of the passive pollutants and obtain a tool able to predict levels of concentrations inside the canyon we made up different CFD models starting from an easy two dimensional model to complex three dimensional ones.

The 2D CFD model gave us much information about the fluid flow behaviour inside of a deep street canyon and about the influence of the main parameters such as the aspect ratio AR = H/W, the wind velocity at roof top level, the background concentration, the vehicular induced turbulence (VIT) and the wind turbulence.

Results show that the wind turbulence has a small effect on the pollutant concentration levels inside the deep street canyon, while background concentration and vehicle induced turbulence have a strong influence.

This model however over estimates pollutant concentrations probably because it doesn't take into account the ventilation effect of the wind velocity component parallel to the street axis.

In order to improve the prediction capability and to take into account this feature we used some three dimensional CFD models. These gave us, levels of concentration inside the canyon, closer to measured during the monitoring campaigns.

In order to investigate on the presence of a lateral and a crossing street to via Nardones and their effects we carried out simulations using two models that we referred as FLUENT-C, i.e. a geometrical complete model, and FLUENT-S, obtained not considering the lateral

and crossing street. Results said us that they don't have a relevant influence but this could be true only for this case where the ratios L/H are quite high.

A geometrical complex three dimensional model, which we refer as M2-C model, was used to reproduce data coming from a monitoring campaign of CO (15th June 2006). Results were in good agreement with measured data. Correlation between them is R = 0.87 that becomes higher if we introduce the VIT effect R = 095.

Three dimensional models give us good results but their application is not easy, you need to set up many parameters, and they are time expensive. Operational model, on the other hand, are easy to use and faster but they are created and tested for regular or near regular street canyon. We used the WinOSPM, which is one of the widely used parametric models, to reproduce data coming from the monitoring campaign of the 15th June 2006.

Results are not very good, correlation between CO measured and CO calculated by this model is low R = 0.52. That is caused by the not adequate representation of the fluid flow inside the deep street canyon.

Analyzing results coming from 3D models we can see that wind velocity at street level obtained by WinOSPM inside the canyon is about ten times higher than that obtained by CFD model.

By applying a further reduction of the street level wind speed by an empirical factor of 10 within the model we obtain a remarkable improvement of the model. Correlation between measured and calculated data increases to R = 0.81. This result is relevant in order to make a parametric model for deep street canyons but we don't know if it's applicable to other street canyons.

References

Favale G., Murena F., Vardoulakis S., Solazzo E., Modelling dispersion of traffic pollution in a deep street canyon: application of CFD and operational models (2008)

Favale G., Murena F., Vardoulakis S., Solazzo E., (2007) Pollutant dispersion in deep street canyons – comparison between CFD and Operational model Simulations, 11th International conference on Harmonization within atmospheric dispersion modelling for regulatory purposes, Cambridge 2-5 July 2007

Hussain M., Lee B.E. An investigation of wind forces on three dimensional roughness elements in a simulated atmospheric boundary layer flow - Part II. Flow over large arrays of identical roughness elements and the effect of frontal and side aspect ratio variations, Report No BS 56, Department of Building Sciences, University of Sheffield (1980).

Isao Kanda, Kiyoshi Uehara, Yukio Yamaoa,Yasuo Yoshikawa, Tazuko Morikawa, A wind-tunnel study on exhaust gas dispersion from road vehicles—Part I: Velocity and concentration fields behind single vehicles, Journal of Wind Engineering and Industrial Aerodynamics 94 639–658 (2006)

Jaakko Kukkonen, Esko Valkonen, Jari Walden, Tarja Koskentalo, Paivi Aarnio, Ari Karppinen, Ruwim Berkowicz, Raimo Kartastenpaa A measurement campaign in a street canyon in Helsinki and comparison of results with predictions of the OSPM model Atmospheric Environment 35 (2001) 231 - 243

Jicha M., Pospisil J., Katolicky J. Dispersion of pollutants in street canyon under traffic induced flow and turbulence, Environmental Monitoring and Assessment, 65 (2000), 343-351

Kastner-Klein P., Berkowicz R., and Plate E.J. Modelling of vehicle induced turbulence in air pollution studies for streets. Journal of Environment and Pollution (1998)

Kastner-Klein P, Berkowicz R, and Britter R. The influence of street architecture on flow and dispersion in street canyons. Meteorol Atmos Phys 87, 121–131 (2004)

Kim, J. and Baik, J. Effects of inflow turbulence intensity on flow and pollutant dispersion in an urban street canyon Journal of wind engineering and industrial aerodynamics 91, 309-329 (2003).

Meroney, R.N., Pavageau, M., Rafailidis, S., Schatzmann, M., 1996. Study of line source characteristic for 2-D physical modelling of pollutant dispersion in street canyons. Journal of Wind Engineering and Industrial Aerodynamics 62, 37-56.

Murena F., Favale G. (2006) Evaluation of passive pollutants residence time in a deep street canyon by CFD simulations 28th NATO/CCMS International Technical Meeting on Air Pollution Modelling and its Application Lipsia

Murena F. and G. Favale, (2007 a) Continuous monitoring of carbon monoxide in a deep street canyon Atmospheric Environment, **41**, 2620-2629

Murena F., Favale G. (2007 b)Comparison of hourly average CO concentration from monitoring and CFD modelling in a Deep Street Canyon, 6th International conference on Urban Air Quality, Cyprus 27-29 March 2007

Murena F., Perna P.P., Vetere L. "L'inquinamento atmosferico nella città di Napoli. Analisi dei dati relativi al CO e allo NO_2", Inquinamento, 14 (2000), 49-55.

Murena F., Vorraro F. "Vertical gradiends of Benzene concentration in a deep street canyon in the urban area of Naples" Atmospheric environment 37 (2003) 4853-4859

Murena F., Garofalo N. and Favale G., Monitoring CO concentration at leeward and windward sides in a deep street canyon, Atmospheric environment (2008) (Submitted)

Nicholson S.E. A pollution model for street–level air, Atmospheric Environment, (1975), 19-31

Ntziachristos, L. Samaras, Z., (2000) COPERT III Computer programme to calculate emissions from road transport - Methodology and emission factors (Version 2.1). European Environment Agency Technical report No 49 November 2000

Oke T.R. Street design and urban canopy layer climate, Energy and Buildings, 11 (1988), 103-113

Plate, E.J. Wind tunnel modelling of wind effects in engineering. Engineering Meteorology. Elsevier, Amsterdam (1982).

Salizzoni, P., Cancelli, C.l, Perkins, R.J., Soulhac, L. & Méjean, P. An experimental study of the influence of a two-scale surface roughness on a turbulent boundary layer 9th Int. Conf. on Harmonisation within Atmospheric Dispersion Modelling for Regulatory Purposes (2004)

Savory E., Rotach, M.W., Chauvet C., Guilleteaou E., Kastner-Klein P., Kovar-Panskus A., Louka P., Sahm P., Trini Castelli S. 2004 "Street architecture and air quality" in Optimisation of modelling methods for traffic pollution in streets TRAPOS by Berkowicz R., Britter R. and Di Sabatino S.

Sini J.-F., Anquetin S., Mestayer P.G. Pollutant dispersion and thermal effects in urban street canyons, Atmospheric Environment, 30 (15) (1996), 2659-2677

Solazzo E., Vardoulakis S., Cai X.,. Evaluation of traffic-producing turbulence schemes within Operational Street Pollution Models using roadside measurements. Atmospheric Environment 41, 5357–5370 (2007).

S. Pal Arya: Air Pollution Meteorology and Dispersion, Oxford University Press, New York, 1999

Soulhac L., Puel C., Duclaux O., Perkins R.J., (2003) Simulations of atmospheric pollution in Greater Lyon an example of the use of nested models Atmospheric Environment 37, 5147-5156

Vardoulakis, S., Fisher, B.E.A., Pericleous, K., Gonzalez-Flesca, N. (2003) Modelling air quality in street canyons: a review. Atmospheric Environment 37, 155 – 182

Vardoulakis, S., Valiantis, M., Milner, M., ApSimon, H. (2007) Operational air pollution modelling in the UK—Street canyon applications and challenges, Atmospheric Environment (41), pp. 4622-4627.

Yamartino, R.J and Wiegand, G. (1986) Development and evaluation of simple models for flow, turbulence and pollutant concentration fields within an urban street canyon, Atmospheric environment, 20, 2137-2156

Ziv, A., Berkowicz, R., Genikhovich, E., Palmgren, F. and Yakovleva, E. (2002) Analysis of the St. Petersburg Traffic Data using the OSPM Model, Water, Air and Soil Pollution: Focus 2(5), pp. 297-310.